 CMES, vol.27, no.3, pp.163-186, 2008

A Differential Reproducing Kernel Particle Method for the Analysis of Multilayered Elastic and Piezoelectric Plates

Chih-Ping Wu[1], **Kuan-Hao Chiu and Yun-Ming Wang**

Abstract: A differential reproducing kernel particle (DRKP) method is proposed and developed for the analysis of simply supported, multilayered elastic and piezoelectric plates by following up the consistent concepts of reproducing kernel particle (RKP) method. Unlike the RKP method in which the shape functions for derivatives of the reproducing kernel (RK) approximants are obtained by directly taking the differentiation with respect to the shape functions of the RK approximants, we construct a set of differential reproducing conditions to determine the shape functions for the derivatives of RK approximants. On the basis of the extended Hellinger-Reissner principle, the Euler-Lagrange equations of three-dimensional piezoelectricity and the possible boundary conditions are derived. A point collocation method based on the present DRKP approximations is formulated for the static analysis of simply supported, multilayered elastic and piezoelectric plates under electro-mechanical loads. It is shown that the present DRKP method indeed is a fully meshless approach with excellent accuracy and fast convergence rate.

Keyword: Meshless methods, Reproducing kernels, Point collocation, Piezoelectric plates, Static, Bending.

1 Introduction

In recent decades, the laminated composite elastic plates bonded with piezoelectric layers on the lateral surfaces of the composite laminates have been designed as the so-called smart (or intelligent) structures. Since the direct and converse effects of the piezoelectric materials, the previously smart structures have been successfully applied in various industries for the purposes of sensing, actuating and controlling. Hence, many theoretical methodologies and numerical modeling have been proposed for the analysis of this new class of smart structures under electro-mechanical loads.

Several two-dimensional (2D) coupled electro-elastic theories have been proposed by extending the basic kinematics assumptions of 2D theories of laminated composite structures to account for the coupled electro-elastic effects. Tauchert (1992) and Tiersten (1969) extended the classical lamination theory (CLT) to study piezothermoelastic and piezoelectric responses of multilayered piezoelectric plates, respectively. Jonnalagadda (1994) and Mindlin (1972) presented the 2D piezothermoelastic and vibration analyses of multilayered piezoelectric plates using an extended first-order shear deformation theory (FSDT), respectively. Khdeir and Aldraihem (2007) proposed an extended higher-order shear deformation theory (HSDT) for the static behavior of laminated composite piezoelectric plates. Shu (2005) presented an accurate theory for the cylindrical bending vibration of laminated piezoelectric plates. Batra and Vidoli (2002) presented a higher-order piezoelectric plate theory derived from a three-dimensional variational principle. Ballhause et al. (2005) proposed a unified formulation for the electro-mechanical analysis of multilayered piezoelectric plates. Various aforementioned 2D coupled theories can be included as the special cases in the unified formulation. The results obtained from various 2D theories have been validated and assessed by comparing these 2D results with 3D solutions available in the literature.

Apart from the aforementioned 2D coupled

[1] Corresponding author. Department of Civil Engineering, National Cheng Kung University, Taiwan, ROC. cpwu@mail.ncku.edu.tw

electro-elastic theories, several three-dimensional (3D) approaches for the exact analysis of laminated piezoelectric plates have also been developed. Following a similar approach as that of Pagano (1969, 1970) for the 3D analysis of laminated composite plates, Heyliger and Brooks (1995, 1996), Heyliger (1994) and Dube et al. (1996) presented the exact cylindrical bending deformation and vibration, electro-elastic and piezo-thermo-elastic analyses of laminated piezoelectric plates, respectively. In conjunction with the state space method, an exact transfer-matrix-based methodology was presented by Lee and Jiang (1996) and Pan (2001, 2003) for the electro-elastic and magneto-electro-elastic analyses of laminated piezoelectric and magneto-electro-elastic plates, respectively. Vel and Batra (2000) presented the 3D analytical solution for hybrid multilayered piezoelectric plates with various boundary conditions. Based on the method of perturbation, Wu and his colleagues (2004, 2006, 2007, 2008) presented the 3D asymptotic solutions for the static and dynamic responses of functionally graded and multilayered piezoelectric plates and shells.

Recently, the meshless method in computational mechanics has considerably attracted the researchers' attention. Liu and his colleagues (1995) proposed a reproducing kernel particle (RKP) method for numerical analysis of partial differential equations. The continuous RKP interpolation functions have been developed by satisfying a set of the reproducing conditions. The RKP method has been applied for the large deformation analysis of non-linear structures (Chen et al., 1996), for metal forming analysis (Chen et al., 1998) and for the dynamic analysis of linear structures (Liu et al., 1995). A point collocation method based on reproducing kernel (RK) approximations has been presented by Aluru (2000). It is shown that Aluru's results for several one and two-dimensional problems are accurate and the convergence rate is fast.

Lancaster and Salkauskas (1981) proposed an alternative approach using the moving least squares (MLS) approximations to develop a meshless method. On a basis of the MLS interpolation functions, several meshless methods have been proposed such as the element-free Galerkin method (Belytschko et al., 1994; Lu et al., 1994), the meshless local Petrov-Galerkin (MLPG) method (Atluri et al., 1999; Atluri and Zhu, 1998, 2000a, 2000b) and the finite point method (Oñate et al., 1996). A comprehensive literature survey on meshless methods has been made by Belytschko et al. (1996).

The MLPG method has been proposed by Atluri and Shen (2002a, b, 2004) for solving various solid mechanics problems. The advantages of this method in comparison with the conventional finite element method, are that the MLPG method does not need to construct any mesh, neither for the interpolation of the field variables nor for the integration of the weak forms. A series of MLPG approaches has been developed by Han and Atluri (2004a, b) for solving the elasto-static and elasto-dynamic problems, respectively. In their formulations, the MLS and the radial basis functions (RBF) are selected as the trial functions and the Heaviside Dirac delta and the Kelvin fundamental elasticity solutions are selected as the test functions. Since the successful applications and excellent performance of the MLPG method to various solid mechanics problems, the MLPG method becomes one of the promising numerical methods for computational mechanics.

Atluri et al. (2004) have proposed a MLPG mixed finite volume method to simplify and speed up the MLPG implementation. In this method, the displacement and stress variables are interpolated using the same shape functions, independently. Consequently, the continuity requirements on the trial functions are reduced by one order and the second derivatives of the shape derivatives of the shape functions are avoided. The MLPG mixed finite volume method was successfully applied to elasto-static problems (Han and Atluri, 2004a), elasto-dynamic problems (Han and Atluri, 2004b) and nonlinear problems (Han et al., 2005).

By using the Dirac delta function as the test function in the MLPG method, Atluri et al. (2006a) have developed a MLPG mixed collocation method for solving elasticity problems. This method has been demonstrated to yield very accurate results with a stable convergence rate. It is concluded that the MLPG mixed collocation method is much more efficient than the MLPG finite volume method. Atluri et al. (2006b) have also proposed a MLPG mixed finite difference method for solid mechanics where the generalized finite difference method is used for approximating the derivatives of a function using the nodal values in the local domain of definition. Numerical examples illustrated that the MLPG mixed finite difference method is suitably used for solving various elasticity problems.

Shu et al. (2003) recently proposed a local RBF-based differential quadrature (DQ) method. In the method, the conventional DQ method is combined with the radial basis functions as the trial functions in the DQ scheme. The local RBF-based DQ method has been successfully applied to study the incompressible flows in the steady and unsteady regions (Shu et al., 2005), two-dimensional incompressible Navier-Stokes equations (Shu et al., 2003), three-dimensional incompressible viscous flows with curved boundary (Shan et al., 2008) and vibration problems of arbitrarily shaped members (Wu et al., 2007).

In the present paper, the attention is placed on the modifications for the derivatives of RK approximants. A novel approach is proposed in the present paper where the shape functions for the derivatives of RK approximants are determined using a set of differential reproducing conditions. That makes the present scheme, namely the differential reproducing kernel particle (DRKP) method, more efficient without directly taking the differentiation with respect to the shape functions of RK approximants. A point collocation method based on the present DRKP approximations is formulated and applied to the 3D electro-elastic analysis of simply supported, multilayered piezoelectric plates under electro-mechanical loads.

2 The Extended Hellinger-Reissner Energy Functional

We consider a simply supported, multilayered elastic and piezoelectric plate as shown in Fig. 1 and subjected to electro-mechanical loads. A Cartesian coordinate system (x_1, x_2 and x_3 coordinates) is adopted and located on the middle surface of the plate. The total thickness of the plate is $2h$; L_1 and L_2 are the in-surface dimensions in the x_1 and x_2 directions, respectively.

The linear constitutive equations valid for the nature of symmetry class of piezoelectric materials are given by

$$\begin{Bmatrix}\sigma_{11}\\ \sigma_{22}\\ \sigma_{33}\\ \sigma_{23}\\ \sigma_{13}\\ \sigma_{12}\end{Bmatrix} = \begin{bmatrix} c_{11} & c_{12} & c_{13} & 0 & 0 & 0\\ c_{12} & c_{22} & c_{23} & 0 & 0 & 0\\ c_{13} & c_{23} & c_{33} & 0 & 0 & 0\\ 0 & 0 & 0 & c_{44} & 0 & 0\\ 0 & 0 & 0 & 0 & c_{55} & 0\\ 0 & 0 & 0 & 0 & 0 & c_{66}\end{bmatrix} \begin{Bmatrix}\varepsilon_{11}\\ \varepsilon_{22}\\ \varepsilon_{33}\\ 2\varepsilon_{23}\\ 2\varepsilon_{13}\\ 2\varepsilon_{12}\end{Bmatrix} - \begin{bmatrix} 0 & 0 & e_{31}\\ 0 & 0 & e_{32}\\ 0 & 0 & e_{33}\\ 0 & e_{24} & 0\\ e_{15} & 0 & 0\\ 0 & 0 & 0\end{bmatrix} \begin{Bmatrix}E_1\\ E_2\\ E_3\end{Bmatrix}, \quad (1)$$

$$\begin{Bmatrix}D_1\\ D_2\\ D_3\end{Bmatrix} = \begin{bmatrix} 0 & 0 & 0 & 0 & e_{15} & 0\\ 0 & 0 & 0 & e_{24} & 0 & 0\\ e_{31} & e_{32} & e_{33} & 0 & 0 & 0\end{bmatrix} \begin{Bmatrix}\varepsilon_{11}\\ \varepsilon_{22}\\ \varepsilon_{33}\\ 2\varepsilon_{23}\\ 2\varepsilon_{13}\\ 2\varepsilon_{12}\end{Bmatrix} + \begin{bmatrix} \eta_{11} & 0 & 0\\ 0 & \eta_{22} & 0\\ 0 & 0 & \eta_{33}\end{bmatrix} \begin{Bmatrix}E_1\\ E_2\\ E_3\end{Bmatrix}, \quad (2)$$

where $\sigma_{11}, \sigma_{22}, \cdots, \sigma_{12}$ are the stress components; ε_{11}, ε_{22}, $\cdots$, ε_{12} are the strain components; D_1, D_2 and D_3 are the electric displacement components; E_1, E_2 and E_3 are the electric field components. c_{ij}, e_{ij} and η_{ij} are the elastic, piezoelectric and dielectric coefficients, respectively, and they are layerwise constants through the thickness coordinate of multilayered plates. For an elastic layer, the corresponding piezoelectric coefficients (e_{ij}) in Eqs. (1)–(2) are zero.

The strain-displacement relations are

$$\varepsilon_{ij} = (u_{i,j} + u_{j,i})/2 \quad (i,\ j = 1,\ 2,\ 3), \tag{3}$$

where u_1, u_2 and u_3 denote the elastic displacement components; the commas denote partial differentiation with respect to the suffix variables.

The electric field-electric potential relations are

$$E_i = -\Phi_{,i} \quad (i = 1,\ 2,\ 3), \tag{4}$$

where Φ denotes the electric potential.

The Hellinger-Reissner (H-R) principle is extended to derive the Euler-Lagrange equations for the coupled-fields analysis of multilayered elastic and piezoelectric plates. The extended H-R energy functional for the problem is in the form

$$\begin{aligned}
\Pi_{HR} = &\int_{-h}^{h}\int_{\Omega}\Big[\sigma_{11}\varepsilon_{11} + \sigma_{22}\varepsilon_{22} + \sigma_{33}\varepsilon_{33} + 2\sigma_{13}\varepsilon_{13} \\
&+ 2\sigma_{23}\varepsilon_{23} + 2\sigma_{12}\varepsilon_{12} + D_1\Phi_{,1} + D_2\Phi_{,2} \\
&+ D_3\Phi_{,3} - B(\sigma_{ij},\ D_i)\Big] dx_1 dx_2 dx_3 \\
&- \int_{\Omega^+} \overline{q}_3^+ u_3 dx_1 dx_2 \\
&- \int_{\Omega^-} \overline{q}_3^- u_3 dx_1 dx_2 \\
&- \delta_{k2}\int_{\Omega^+} \overline{D}_3^+ \Phi dx_1 dx_2 \\
&- \delta_{k1}\int_{\Omega^+} D_3(\Phi - \overline{\Phi}^+) dx_1 dx_2 \\
&- \delta_{k2}\int_{\Omega^-} \overline{D}_3^- \Phi dx_1 dx_2 \\
&- \delta_{k1}\int_{\Omega^-} D_3(\Phi - \overline{\Phi}^-) dx_1 dx_2 \\
&- \int_{-h}^{h}\int_{\Gamma_\sigma} \overline{T}_i u_i d\Gamma dx_3 \\
&- \int_{-h}^{h}\int_{\Gamma_u} T_i(u_i - \overline{u}_i) d\Gamma dx_3 \\
&- \int_{-h}^{h}\int_{\Gamma_D} \overline{D}_n \Phi d\Gamma dx_3 \\
&- \int_{-h}^{h}\int_{\Gamma_\Phi} D_n(\Phi - \overline{\Phi}) d\Gamma dx_3,
\end{aligned} \tag{5}$$

where δ_{kl} is called the Kronecker delta; as the subscripts $k = l$=1 (or $k = l$=2), it represents the electric potential (or the normal electric displacement) is prescribed on the lateral surfaces;Ω denotes the plate domain on the $x_1 - x_2$ plane; Ω^+ and Ω^- denote the top surface ($x_3 = h$) and bottom surface ($x_3 = -h$) of the plate where the transverse loads $\overline{q}_3^{\pm}$ and either the electric potential $\overline{\Phi}^{\pm}$ (k=1) or the electric displacement $\overline{D}_3^{\pm}$ (k=2) are applied. Γ_σ, Γ_u, Γ_D and Γ_Φ denote the portions of the edge boundary where the surface tractions $\overline{T}_i$, the surface displacements $\overline{u}_i$, the surface charge $\overline{D}_n$ and the surface electric potential $\overline{\Phi}$ are prescribed, repectively. $B(\sigma_{ij}, D_i)$ is the complementary electric enthalpy density function.

In the present formulation, we take the elastic displacements, the transverse stresses, the normal electric displacement and the electric potential to be the primary variables subject to variation. The strains, electric fields, in-plane stresses and in-plane electric displacements are then the dependent variables. They can be expressed in terms of the primary variables using Eqs. (1)-(4) and given as follows:

$$\varepsilon_{11} = \partial B/\partial\sigma_{11} = u_{1,1}, \tag{6}$$

$$\varepsilon_{22} = \partial B/\partial\sigma_{22} = u_{2,2}, \tag{7}$$

$$\varepsilon_{33} = \partial B/\partial\sigma_{33} = -a_1 u_{1,1} - a_2 u_{2,2} + \overline{\eta}\sigma_{33} + \overline{e}D_3, \tag{8}$$

$$2\varepsilon_{13} = \partial B/\partial\sigma_{13} = c_{55}^{-1}\sigma_{13} - c_{55}^{-1}e_{15}\Phi_{,1}, \tag{9}$$

$$2\varepsilon_{23} = \partial B/\partial\sigma_{23} = c_{44}^{-1}\sigma_{23} - c_{44}^{-1}e_{24}\Phi_{,2}, \tag{10}$$

$$2\varepsilon_{12} = \partial B/\partial\sigma_{12} = u_{1,2} + u_{2,1}, \tag{11}$$

$$E_1 = -\partial B/\partial D_1 = -\Phi_{,1}, \tag{12}$$

$$E_2 = -\partial B/\partial D_2 = -\Phi_{,2}, \tag{13}$$

$$E_3 = -\partial B/\partial D_3 = b_1 u_{1,1} + b_2 u_{2,2} - \overline{e}\sigma_{33} + \overline{c}D_3, \tag{14}$$

$$\begin{Bmatrix}\sigma_{11}\\ \sigma_{22}\\ \sigma_{12}\end{Bmatrix} = \begin{bmatrix} Q_{11}\partial_1 & Q_{12}\partial_2 \\ Q_{21}\partial_1 & Q_{22}\partial_2 \\ Q_{66}\partial_2 & Q_{66}\partial_1 \end{bmatrix}\begin{Bmatrix}u_1\\ u_2\end{Bmatrix} + \begin{bmatrix}a_1\\ a_2\\ 0\end{bmatrix}\sigma_{33}$$

$$+\begin{bmatrix} b_1 \\ b_2 \\ 0 \end{bmatrix} D_3, \quad (15)$$

$$\begin{Bmatrix} D_1 \\ D_2 \end{Bmatrix} = \begin{bmatrix} c_{55}^{-1}e_{15} & 0 \\ 0 & c_{44}^{-1}e_{24} \end{bmatrix} \begin{Bmatrix} \sigma_{13} \\ \sigma_{23} \end{Bmatrix} - \begin{bmatrix} (c_{55}^{-1}e_{15}^2+\eta_{11})\partial_1 \\ (c_{44}^{-1}e_{24}^2+\eta_{22})\partial_2 \end{bmatrix} \Phi, \quad (16)$$

where

$a_i = (e_{33}e_{3i}+\eta_{33}c_{i3})/(\eta_{33}c_{33}+e_{33}^2)$,

$b_i = (e_{33}c_{i3}-c_{33}e_{3i})/(\eta_{33}c_{33}+e_{33}^2)$,

$Q_{ij} = c_{ij}-a_jc_{i3}-b_je_{3i}\ (i,j=1,2,6),\ Q_{ij}\neq Q_{ji}$,

$\overline{\eta} = \eta_{33}/(\eta_{33}c_{33}+e_{33}^2)$,

$\overline{e} = e_{33}/(\eta_{33}c_{33}+e_{33}^2)$,

$\overline{c} = c_{33}/(\eta_{33}c_{33}+e_{33}^2)$.

3 Euler-Lagrange equations of 3D piezoelectricity

Substituting Eqs. (6)-(16) into Eq. (5) and imposing the stationary principle of the extended H-R energy functional (i.e., $\delta\Pi_{HR}=0$) yields

$$\begin{aligned}
&\delta\Pi_{HR} = \\
&\int_{-h}^{h}\int_{\Omega}\Big\{\sigma_{11}\delta u_{1,1}+\sigma_{22}\delta u_{2,2} \\
&+\sigma_{12}(\delta u_{1,2}+\delta u_{2,1})+\sigma_{33}\delta u_{3,3} \\
&+\sigma_{23}(\delta u_{3,2}+\delta u_{2,3})+\sigma_{13}(\delta u_{3,1}+\delta u_{1,3}) \\
&+D_1\delta\Phi_{,1}+D_2\delta\Phi_{,2}+D_3\delta\Phi_{,3} \\
&+[u_{3,3}-(-a_1u_{1,1}-a_2u_{2,2}+\overline{\eta}\sigma_{33}+\overline{e}D_3)]\delta\sigma_{33} \\
&+[u_{2,3}+u_{3,2}-(c_{44}^{-1}\sigma_{23}-c_{44}^{-1}e_{24}\Phi,2)]\delta\sigma_{23} \\
&+[u_{1,3}+u_{3,1}-(c_{55}^{-1}\sigma_{13}-c_{55}^{-1}e_{15}\Phi,1)]\delta\sigma_{13} \\
&+[\Phi_{,3}-(-b_1u_{1,1}-b_2u_{2,2}+\overline{e}\sigma_{33}-\overline{c}D_3)]\delta D_3\Big\} \\
&dx_1dx_2dx_3 \\
&-\int_{\Omega^+}\overline{q}_3^+\delta u_3dx_1dx_2 \\
&-\int_{\Omega^-}\overline{q}_3^-\delta u_3dx_1dx_2 \\
&-\delta_{k2}\int_{\Omega^+}\overline{D}_3^+\delta\Phi dx_1dx_2 \\
&-\delta_{k1}\int_{\Omega^+}\delta D_3(\Phi-\overline{\Phi}^+)dx_1dx_2 \\
&-\delta_{k2}\int_{\Omega^-}\overline{D}_3^-\delta\Phi dx_1dx_2 \\
&-\delta_{k1}\int_{\Omega^-}\delta D_3(\Phi-\overline{\Phi}^-)dx_1dx_2 \\
&-\int_{-h}^{h}\int_{\Gamma_\sigma}\overline{T}_i\delta u_id\Gamma dx_3 \\
&-\int_{-h}^{h}\int_{\Gamma_u}\delta T_i(u_i-\overline{u}_i)d\Gamma dx_3 \\
&-\int_{-h}^{h}\int_{\Gamma_D}\overline{D}_n\delta\Phi d\Gamma dx_3 \\
&-\int_{-h}^{h}\int_{\Gamma_\Phi}\delta D_n(\Phi-\overline{\Phi})d\Gamma dx_3 \\
&=0.
\end{aligned} \quad (17)$$

After performing the integration by parts and using Green's theorem, we obtain the Euler-Lagrange equations of 3D piezoelectricity from the domain integral terms and the admissible boundary conditions from the boundary integral terms. They are written as follows:

For Euler-Lagrange equations,

$$\delta u_1: \quad \sigma_{13,3} = -\sigma_{11,1}-\sigma_{12,2}, \quad (18)$$

$$\delta u_2: \quad \sigma_{23,3} = -\sigma_{12,1}-\sigma_{22,2}, \quad (19)$$

$$\delta u_3: \quad \sigma_{33,3} = -\sigma_{13,1}-\sigma_{23,2}, \quad (20)$$

$$\delta\sigma_{13}: \quad u_{1,3} = -u_{3,1}+c_{55}^{-1}\sigma_{13}-c_{55}^{-1}e_{15}\Phi_{,1}, \quad (21)$$

$$\delta\sigma_{23}: \quad u_{2,3} = -u_{3,2}+c_{44}^{-1}\sigma_{23}-c_{44}^{-1}e_{24}\Phi_{,2}, \quad (22)$$

$$\delta\sigma_{33}: \quad u_{3,3} = -a_1u_{1,1}-a_2u_{2,2}+\overline{\eta}\sigma_{33}+\overline{e}D_3, \quad (23)$$

$$\delta D_3: \quad \Phi_{,3} = -b_1u_{1,1}-b_2u_{2,2}+\overline{e}\sigma_{33}-\overline{c}D_3, \quad (24)$$

$$\delta\Phi: \quad D_{3,3} = -D_{1,1}-D_{2,2}. \quad (25)$$

For the lateral boundary conditions,

$$\begin{bmatrix}\sigma_{13} & \sigma_{23}\end{bmatrix} = \begin{bmatrix}0 & 0\end{bmatrix} \text{ on } x_3=\pm h, \quad (26a)$$

$$\sigma_{33}=\overline{q}_3^+(x_1,x_2)$$
$$\text{and (either } D_3=\overline{D}_3^+(x_1,x_2)$$
$$\text{or } \Phi=\overline{\Phi}^+(x_1,x_2)) \text{ on } x_3=h, \quad (26b)$$

$$\sigma_{33}=-\overline{q}_3^-(x_1,x_2)$$
$$\text{and (either } D_3=-\overline{D}_3^-(x_1,x_2)$$
$$\text{or } \Phi=-\overline{\Phi}^-(x_1,x_2)) \text{ on } x_3=-h. \quad (26c)$$

The edge boundary conditions are

$$\sigma_{11}n_1+\sigma_{12}n_2=\overline{T}_1 \text{ or } u_1=\overline{u}_1, \quad (27a)$$
$$\sigma_{12}n_1+\sigma_{22}n_2=\overline{T}_2 \text{ or } u_2=\overline{u}_2, \quad (27b)$$
$$\sigma_{13}n_1+\sigma_{23}n_2=\overline{T}_3 \text{ or } u_3=\overline{u}_3, \quad (27c)$$
$$D_1n_1+D_2n_2=\overline{D}_n \text{ or } \Phi=\overline{\Phi}. \quad (27d)$$

Using Eqs. (6)-(16), we can rewrite the previous Euler-Lagrange equations in terms of the primary variables and its matrix form is given as

$$\begin{Bmatrix} u_{1,3} \\ u_{2,3} \\ \sigma_{33,3} \\ D_{3,3} \\ \sigma_{13,3} \\ \sigma_{23,3} \\ u_{3,3} \\ \Phi_{,3} \end{Bmatrix} = \begin{bmatrix} 0 & 0 & 0 & 0 & d_{15} & 0 & d_{17} & d_{18} \\ 0 & 0 & 0 & 0 & 0 & d_{26} & d_{27} & d_{28} \\ 0 & 0 & 0 & 0 & d_{17} & d_{27} & 0 & 0 \\ 0 & 0 & 0 & 0 & d_{18} & d_{28} & 0 & d_{48} \\ d_{51} & d_{52} & d_{53} & d_{54} & 0 & 0 & 0 & 0 \\ d_{61} & d_{62} & d_{63} & d_{64} & 0 & 0 & 0 & 0 \\ d_{53} & d_{63} & d_{73} & d_{74} & 0 & 0 & 0 & 0 \\ d_{54} & d_{64} & d_{74} & d_{84} & 0 & 0 & 0 & 0 \end{bmatrix} \begin{Bmatrix} u_1 \\ u_2 \\ \sigma_{33} \\ D_3 \\ \sigma_{13} \\ \sigma_{23} \\ u_3 \\ \Phi \end{Bmatrix}, \quad (28)$$

where

$$d_{15}=c_{55}^{-1}, \quad d_{17}=-\partial_1, \quad d_{18}=-c_{55}^{-1}e_{15}\partial_1,$$
$$d_{26}=c_{44}^{-1}, \quad d_{27}=-\partial_2, \quad d_{28}=-c_{44}^{-1}e_{24}\partial_2,$$
$$d_{48}=(c_{55}^{-1}e_{15}^2+\eta_{11})\partial_{11}+(c_{44}^{-1}e_{24}^2+\eta_{22})\partial_{22},$$
$$d_{51}=-(Q_{11}\partial_{11}+Q_{66}\partial_{22}),$$
$$d_{52}=-(Q_{12}+Q_{66})\partial_{12},$$
$$d_{53}=-a_1\partial_1, \quad d_{54}=-b_1\partial_1,$$
$$d_{61}=-(Q_{21}+Q_{66})\partial_{12},$$
$$d_{62}=-(Q_{66}\partial_{11}+Q_{22}\partial_{22}),$$
$$d_{63}=-a_2\partial_2, \quad d_{64}=-b_2\partial_2,$$
$$d_{73}=\overline{\eta}, \quad d_{74}=\overline{e}, \quad d_{83}=\overline{e}, \quad d_{84}=-\overline{c}.$$

The set of Euler-Lagrange equations (Eq. (28)) associated with a set of appropriate boundary conditions (Eqs. (26)-(27)) are composed of a well-posed boundary value problem. Here, a differential reproducing kernel particle method is newly proposed to solve this boundary value problem corresponding to the static behavior of simply supported, multilayered elastic and piezoelectric plates under electro-mechanical loads.

4 A DRKP approximation scheme

4.1 Reproducing kernel shape functions

To solve the differential equation system governing a certain physical problem more efficient, we aim at developing the continuous shape functions for the derivatives of RK approximants associated with each discrete point in the domain (Ω) by following up the consistent concepts of RKP method (Liu et al., 1995). In order to make a clear interpretation, we simplify the derivation of the present scheme for one-dimensional problems.

It is assumed that there are NP discrete points randomly selected and located at x_1, $x_2, \cdots, x_{NP}$, respectively, in the domain. The reproducing kernel approximant $u^a(x)$ of unknown function $u(x)$, $\forall\, x\in\Omega$, is defined as

$$u^a(x)=\sum_{l=1}^{NP}\phi_l(x)\hat{u}_l, \quad (29)$$

where $\phi_l(x)=w_a(x-x_l)C(x;x-x_l)$,

$C(x;\, x-x_l)=\mathbf{P}^T(x-x_l)\,\mathbf{b}(x)$,

$\mathbf{P}^T(x-x_l) =$
$$\begin{bmatrix} 1 & (x-x_l) & (x-x_l)^2 & \cdots & (x-x_l)^n \end{bmatrix},$$

$\mathbf{b}^T(x) = \begin{bmatrix} b_0(x) & b_1(x) & b_2(x) & \cdots & b_n(x) \end{bmatrix}$;

$\hat{u}_l(l = 1, 2, \cdots, NP)$ are the fictitious nodal values and are not the nodal values of $u^a(x)$ in general; $\phi_l(x)$ is the reproducing kernel shape functions corresponding to nodal point at $x = x_l$; $w_a(x-x_l)$ is the weight function centered at x_l with a support size a, $C(x; x-x_l)$ is the correction function; $b_j(x)$ $(j = 0, 1, 2, \cdots, n)$ are the undetermined functions and will be determined by satisfying the reproducing conditions, and n is the highest order of the basis functions.

By selecting the complete n^{th}-order polynomials as the basis functions to be reproduced, we obtain a set of reproducing conditions to determine the undetermined functions of $b_l(x)$ in Eq. (29). The reproducing conditions are give as

$$\sum_{l=1}^{NP} \phi_l(x) x_l^m = x^m \quad m = 0,\ 1,\ 2,\ \cdots,\ n. \tag{30}$$

Equation (30) represents (n+1) reproducing conditions and can be rearranged in the explicit form as follows:

$$m = 0: \ \sum_{l=1}^{NP} \phi_l(x) = 1, \tag{31}$$

$$\begin{aligned} m = 1: \ & \sum_{l=1}^{NP} \phi_l(x)\,(x-x_l) \\ & = x\sum_{l=1}^{NP} \phi_l(x) - \sum_{l=1}^{NP} \phi_l(x) x_l = 0, \end{aligned} \tag{32}$$

$$\begin{aligned} m = 2: \ & \sum_{l=1}^{NP} \phi_l(x)(x-x_l)^2 \\ = x^2 & \sum_{l=1}^{NP} \phi_l(x) - 2x\sum_{l=1}^{NP} \phi_l(x) x_l + \sum_{l=1}^{NP} \phi_l(x) x_l^2 = 0, \end{aligned} \tag{33}$$

$$\vdots$$

$$m = n: \ \sum_{l=1}^{NP} \phi_l(x)(x-x_l)^n = 0. \tag{34}$$

The matrix form of the previous reproducing conditions is given as

$$\begin{aligned} & \sum_{l=1}^{NP} \mathbf{P}(x-x_l)\phi_l(x) \\ & = \sum_{l=1}^{NP} \mathbf{P}(x-x_l) w_a(x-x_l) \mathbf{P}^T(x-x_l) \mathbf{b}(x) \\ & = \mathbf{P}(0) \end{aligned} \tag{35}$$

where $\mathbf{P}(0) = \begin{bmatrix} 1 & 0 & 0 & \cdots & 0 \end{bmatrix}^T$.

According to the reproducing conditions (Eq. (7)), we may obtain the undetermined function matrix $\mathbf{b}(x)$ in the following form

$$\mathbf{b}(x) = \mathbf{A}^{-1}(x)\,\mathbf{P}(0), \tag{36}$$

where $\mathbf{A}(x) = \sum_{l=1}^{NP} \mathbf{P}(x-x_l) w_a(x-x_l) \mathbf{P}^T(x-x_l)$.

Substituting Eq. (36) into Eq. (29) yields the reproducing kernel shape functions in the form of

$$\phi_l(x) = w_a(x-x_l)\mathbf{P}^T(x-x_l)\mathbf{A}^{-1}(x)\mathbf{P}(0). \tag{37}$$

It is realized from Eq. (37) that $\phi_l(x)$ vanishes when x is not in the support of nodal point at $x = x_l$. The influence of the shape functions in the support of the referred nodal point monotonically decreases as the relative distance to the nodal point increases. The fact preserves the local character of the present scheme.

4.2 Derivatives of reproducing kernel shape functions

Since the reproducing kernel approximant $u^a(x)$ is given in Eq. (29), the first derivative of $u^a(x)$ is therefore expressed as

$$\frac{du^a(x)}{dx} = \sum_{l=1}^{NP} \phi_l^{(1)}(x)\hat{u}_l, \tag{38}$$

where $\phi_l^{(1)}(x)$ denote the first-order derivatives of the shape functions.

In the conventional RKP method, $\phi_l^{(1)}(x)$ $(l = 1,\ 2, \cdots, NP)$ are obtained by directly taking the differential operation toward the shape functions of the approximants $\phi_l(x)$. That results in the lengthy expression and complicated computation, especially for the calculation involving the higher-order derivatives of the approximant. Contrary to the aforementioned manipulation, a novel approach is proposed in the paper. The shape functions for the derivatives of approximants are determined using a set of differential reproducing conditions. The detailed derivation is given as follows.

In the present scheme, we express $\phi_l^{(1)}(x)$ in the similar form of $\phi_l(x)$ and given as

$$\phi_l^{(1)}(x) = w_a(x-x_l)\, C_1(x;\, x-x_l), \tag{39}$$

where $C_1(x;\, x-x_l) = \mathbf{P}^T(x-x_l)\, \mathbf{b}_1(x)$,

$$\mathbf{b}_1^T(x) = \begin{bmatrix} b_0^1(x) & b_1^1(x) & b_2^1(x) & \cdots & b_n^1(x) \end{bmatrix}.$$

The differential reproducing conditions for a set of complete n^{th}-order polynomials are given as

$$\sum_{l=1}^{NP} \phi_l^{(1)}(x)\, x_l^m = m x^{m-1} \quad m = 0,\ 1,\ 2,\ \cdots,\ n. \tag{40}$$

Equation (40) can be rearranged and explicitly written as follows:

$$m = 0: \ \sum_{l=1}^{NP} \phi_l^{(1)}(x) = 0, \tag{41}$$

$$\begin{aligned} m = 1: \ & \sum_{l=1}^{NP} \phi_l^{(1)}(x)\, (x-x_l) \\ & = x\sum_{l=1}^{NP} \phi_l^{(1)}(x) - \sum_{l=1}^{NP} \phi_l^{(1)}(x) x_l = -1, \end{aligned} \tag{42}$$

$$\begin{aligned} m = 2: \ & \sum_{l=1}^{NP} \phi_l^{(1)}(x)\, (x-x_l)^2 \\ = x^2 & \sum_{l=1}^{NP} \phi_l^{(1)}(x) - 2x\sum_{l=1}^{NP} \phi_l^{(1)}(x) x_l + \sum_{l=1}^{NP} \phi_l^{(1)}(x) x_l^2 = 0, \end{aligned} \tag{43}$$

$\vdots$

$$m = n: \ \sum_{l=1}^{NP} \phi_l^{(1)}(x)\, (x-x_l)^n = 0. \tag{44}$$

The matrix form of the differential reproducing conditions is given as

$$\begin{aligned} & \sum_{l=1}^{NP} \mathbf{P}(x-x_l)\phi_l^{(1)}(x) \\ & = \sum_{l=1}^{NP} \mathbf{P}(x-x_l) w_a(x-x_l) \mathbf{P}^T(x-x_l) \mathbf{b}_1(x) \\ & \qquad = -\mathbf{P}^{(1)}(0), \end{aligned} \tag{45}$$

where $(-1)\left[\mathbf{P}^{(1)}(0)\right] = -\left.\frac{d\mathbf{P}(x-x_l)}{dx}\right|_{x=x_l} = \begin{bmatrix} 0 & -1 & 0 & \cdots & 0 \end{bmatrix}^T$.

The undetermined function matrix $\mathbf{b}_1(x)$ can then be obtained and given by

$$\mathbf{b}_1(x) = -\mathbf{A}^{-1}(x)\, \mathbf{P}^{(1)}(0). \tag{46}$$

Substituting Eq. (46) into Eq. (39) yields the first-order derivative of the reproducing kernel shape functions in the form of

$$\phi_l^{(1)}(x) = -w_a(x-x_l)\mathbf{P}^T(x-x_l)\mathbf{A}^{-1}(x)\mathbf{P}^{(1)}(0). \tag{47}$$

Carrying on the similar derivation to the k^{th}-order derivative of the reproducing kernel approximant leads to

$$\frac{d^k u^a(x)}{dx^k} = \sum_{l=1}^{NP} \phi_l^{(k)}(x)\hat{u}_l, \tag{48}$$

where

$$\begin{aligned} & \phi_l^{(k)}(x) = \\ & \qquad (-1)^k w_a(x-x_l)\mathbf{P}^T(x-x_l)\mathbf{A}^{-1}(x)\mathbf{P}^{(k)}(0), \end{aligned}$$

$$\mathbf{P}^{(k)}(0) = \left.\frac{d^k\mathbf{P}(x-x_l)}{dx^k}\right|_{x=x_l}.$$

It is found from observing Eqs. (37), (47) and (48) that the shape functions of reproducing kernel approximant and its derivatives are independent of one another and easy to be applied in the point collocation method.

4.3 Weight functions

In implementing the present scheme, the weight functions must be selected in advance. The conventional weight function of cubic spline is used in the present analysis and given as

Cubic spline: $w_a(x-x_l) = w(s) =$

$$\begin{cases} 4s^3 - 4s^2 + (2/3) & \text{for } s \le (1/2) \\ -(4/3)s^3 + 4s^2 - 4s + (4/3) & \text{for } (1/2) < s \le 1 \\ 0 & \text{for } s > 1 \end{cases}, \tag{49}$$

where $s = |x-x_l|/a$.

It is noted that a very small value of a may result in an ill-conditioned problem since the system matrix $\mathbf{A}(x)$ will becomes singular. On the other hand, the value of a also has to be small enough to preserve the local character of the present scheme. Hence, a compromise range of the value of a has to be studied later to ensure the accuracy and convergence of the present scheme.

5 Applications

Based on the proposed differential reproducing kernel particle scheme, a point collocation method is used for the coupled analysis of simply supported, multilayered elastic and piezoelectric plates. The loading conditions on the top and bottom surfaces and edge boundary conditions of the plate are given as follows:

The loading conditions of the plates are

$$\begin{aligned} \overline{q}_3^+ &= q_0^+ \sin(\hat{m}\pi x_1/L_1)\sin(\hat{n}\pi x_2/L_2), \\ \overline{q}_3^- &= q_0^- \sin(\hat{m}\pi x_1/L_1)\sin(\hat{n}\pi x_2/L_2); \end{aligned} \tag{50}$$

either

$$\begin{aligned} \overline{D}_3^+ &= D_0^+ \sin(\hat{m}\pi x_1/L_1)\sin(\hat{n}\pi x_2/L_2), \\ \overline{D}_3^- &= D_0^- \sin(\hat{m}\pi x_1/L_1)\sin(\hat{n}\pi x_2/L_2), \end{aligned} \tag{51a}$$

or,

$$\overline{\Phi}^+ = \Phi_0^+ \sin(\hat{m}\pi x_1/L_1)\sin(\hat{n}\pi x_2/L_2). \tag{51b}$$

where $\hat{m}$ and $\hat{n}$ are the wave numbers along the x_1 and x_2 coordinates, respectively.

The edge boundary conditions of the plates are considered as the fully simple supports and suitably grounded and written as

$$u_2 = u_3 = \sigma_{11} = \Phi = 0 \text{ at } x_1 = 0 \text{ and } L_1, \tag{52a}$$

$$u_1 = u_3 = \sigma_{22} = \Phi = 0 \text{ at } x_2 = 0 \text{ and } L_2. \tag{52b}$$

For making the calculation more efficient and preventing from the ill-conditioned of system matrix, we select a set of dimensionless variables to normalize the coordinates and the variables of electric and elastic fields. The dimensionless variables are given as

$$x = x_1/L, \quad y = x_2/L, \quad z = x_3/h; \tag{53a}$$

$$u = u_1/h, \quad v = u_2/h, \quad w = u_3/L; \tag{53b}$$

$$\begin{aligned} &\sigma_x = L\sigma_{11}/(hQ), \quad \sigma_y = L\sigma_{22}/(hQ), \\ &\sigma_{xy} = L\sigma_{12}/(hQ); \end{aligned} \tag{53c}$$

$$\begin{aligned} &\sigma_{xz} = L^2\sigma_{13}/h^2Q, \quad \sigma_{yz} = L^2\sigma_{23}/h^2Q, \\ &\sigma_z = L^3\sigma_{33}/h^3Q; \end{aligned} \tag{53d}$$

$$\begin{aligned} &D_x = hD_1/(Le), \quad D_y = hD_2/(Le), \\ &D_z = LD_3/(he); \end{aligned} \tag{53e}$$

$$\phi = Le\Phi/(h^2Q); \tag{53f}$$

where L denotes a typical in-plane dimension of the plate and is taken to be $L = \sqrt{L_1L_2}$ in the paper; $-1 \le z \le 1$; e and Q stand for a reference piezoelectric and elastic modulus; Q is taken as $Q = (1/2h)\int_{-h}^{h} c_{33}dx_3$.

The method of double Fourier series expansion is firstly applied to reduce the system of partial differential equations (Eq. (28)) to a system of ordinary differential equations. By satisfying the edge boundary conditions, we express the primary variables in the following form

$$u = \sum_{\hat{m}=1}^{\infty}\sum_{\hat{n}=1}^{\infty} u_{\hat{m}\hat{n}}(z)\cos\tilde{m}x\sin\tilde{n}y, \tag{54}$$

$$v = \sum_{\hat{m}=1}^{\infty}\sum_{\hat{n}=1}^{\infty} v_{\hat{m}\hat{n}}(z)\sin\tilde{m}x\cos\tilde{n}y, \tag{55}$$

$$w = \sum_{\hat{m}=1}^{\infty}\sum_{\hat{n}=1}^{\infty} w_{\hat{m}\hat{n}}(z)\sin\tilde{m}x\sin\tilde{n}y, \tag{56}$$

$$\tau_{xz} = \sum_{\hat{m}=1}^{\infty}\sum_{\hat{n}=1}^{\infty} \tau_{xz\hat{m}\hat{n}}(z)\cos\tilde{m}x\sin\tilde{n}y, \tag{57}$$

$$\tau_{yz}=\sum_{\hat{m}=1}^{\infty}\sum_{\hat{n}=1}^{\infty}\tau_{yz\hat{m}\hat{n}}(z)\sin\tilde{m}x\cos\tilde{n}y, \tag{58}$$

$$\sigma_z=\sum_{\hat{m}=1}^{\infty}\sum_{\hat{n}=1}^{\infty}\sigma_{z\hat{m}\hat{n}}(z)\sin\tilde{m}x\sin\tilde{n}y, \tag{59}$$

$$D_z=\sum_{\hat{m}=1}^{\infty}\sum_{\hat{n}=1}^{\infty}D_{z\hat{m}\hat{n}}(z)\sin\tilde{m}x\sin\tilde{n}y, \tag{60}$$

$$\phi=\sum_{\hat{m}=1}^{\infty}\sum_{\hat{n}=1}^{\infty}\phi_{\hat{m}\hat{n}}(z)\sin\tilde{m}x\sin\tilde{n}y, \tag{61}$$

where $\tilde{m}=\hat{m}\pi L/L_1$ and $\tilde{n}=\hat{n}\pi L/L_2$.

For brevity, the symbols of summation are omitted in the following derivation. By using the set of dimensionless coordinates and field variables ((Eq. (53)) and substituting the Eqs. (54)-(61) in the Euler-Lagrange equations (Eq. (28)), we have the resulting equations as follows:

$$\begin{Bmatrix} u_{\hat{m}\hat{n},z}\\ v_{\hat{m}\hat{n},z}\\ \sigma_{z\hat{m}\hat{n},z}\\ D_{z\hat{m}\hat{n},z}\\ \sigma_{xz\hat{m}\hat{n},z}\\ \sigma_{yz\hat{m}\hat{n},z}\\ w_{\hat{m}\hat{n},z}\\ \phi_{\hat{m}\hat{n},z}\end{Bmatrix}=\begin{bmatrix} 0&0&0&0&\tilde{d}_{15}&0&\tilde{d}_{17}&\tilde{d}_{18}\\ 0&0&0&0&0&\tilde{d}_{26}&\tilde{d}_{27}&\tilde{d}_{28}\\ 0&0&0&0&-\tilde{d}_{17}&-\tilde{d}_{27}&0&0\\ 0&0&0&0&-\tilde{d}_{18}&-\tilde{d}_{28}&0&\tilde{d}_{48}\\ \tilde{d}_{51}&\tilde{d}_{52}&\tilde{d}_{53}&\tilde{d}_{54}&0&0&0&0\\ \tilde{d}_{61}&\tilde{d}_{62}&\tilde{d}_{63}&\tilde{d}_{64}&0&0&0&0\\ -\tilde{d}_{53}&-\tilde{d}_{63}&\tilde{d}_{73}&\tilde{d}_{74}&0&0&0&0\\ -\tilde{d}_{54}&-\tilde{d}_{64}&\tilde{d}_{74}&\tilde{d}_{84}&0&0&0&0\end{bmatrix}\begin{Bmatrix} u_{\hat{m}\hat{n}}\\ v_{\hat{m}\hat{n}}\\ \sigma_{z\hat{m}\hat{n}}\\ D_{z\hat{m}\hat{n}}\\ \sigma_{xz\hat{m}\hat{n}}\\ \sigma_{yz\hat{m}\hat{n}}\\ w_{\hat{m}\hat{n}}\\ \phi_{\hat{m}\hat{n}}\end{Bmatrix}, \tag{62}$$

where

$$\tilde{d}_{15}=Qh^2/c_{55}L^2,\quad \tilde{d}_{17}=-\tilde{m},$$
$$\tilde{d}_{18}=-Qe_{15}h^2\tilde{m}/c_{55}e_0L^2,$$
$$\tilde{d}_{26}=Qh^2/c_{44}L^2,\quad \tilde{d}_{27}=-\tilde{n},$$
$$\tilde{d}_{28}=-Qe_{24}h^2\tilde{n}/c_{44}e_0L^2,$$

$$\tilde{d}_{48}=-(c_{55}^{-1}e_{15}^2+\eta_{11})(Qh^2/e_0^2L^2)\tilde{m}^2 - (c_{44}^{-1}e_{24}^2+\eta_{22})(Qh^2/e_0^2L^2)\tilde{n}^2,$$

$$\tilde{d}_{51}=(\tilde{Q}_{11}\tilde{m}^2+\tilde{Q}_{66}\tilde{n}^2),\quad \tilde{d}_{52}=(\tilde{Q}_{12}+\tilde{Q}_{66})\tilde{m}\tilde{n},$$
$$\tilde{d}_{53}=-a_1(h^2/L^2)\tilde{m},\quad \tilde{d}_{54}=-b_1(e_0/Q)\tilde{m},$$
$$\tilde{d}_{61}=(\tilde{Q}_{21}+\tilde{Q}_{66})\tilde{m}\tilde{n},\quad \tilde{d}_{62}=(\tilde{Q}_{66}\tilde{m}^2+\tilde{Q}_{22}\tilde{n}^2),$$
$$\tilde{d}_{63}=-a_2(h^2/L^2)\tilde{n},\quad \tilde{d}_{64}=-b_2(e_0/Q)\tilde{n},$$
$$\tilde{d}_{73}=\overline{\eta}Q(h^4/L^4),\quad \tilde{d}_{74}=\overline{e}e_0h^2/L^2,$$
$$\tilde{d}_{81}=b_1(e_0/Q)\tilde{m},\quad \tilde{d}_{82}=b_2(e_0/Q)\tilde{n},$$
$$\tilde{d}_{83}=\overline{e}e_0h^2/L^2,\quad \tilde{d}_{84}=-\overline{c}e_0^2/Q.$$

Similarly, the dimensionless dependent variables of in-plane stresses and in-plane electric displacements can be expressed in terms of the primary variables as follows:

$$\sigma_x=\sum_{\hat{m}=1}^{\infty}\sum_{\hat{n}=1}^{\infty}\sigma_{x\hat{m}\hat{n}}(z)\sin\tilde{m}x\sin\tilde{n}y, \tag{63}$$

$$\sigma_y=\sum_{\hat{m}=1}^{\infty}\sum_{\hat{n}=1}^{\infty}\sigma_{y\hat{m}\hat{n}}(z)\sin\tilde{m}x\sin\tilde{n}y, \tag{64}$$

$$\sigma_{xy}=\sum_{\hat{m}=1}^{\infty}\sum_{\hat{n}=1}^{\infty}\sigma_{xy\hat{m}\hat{n}}(z)\cos\tilde{m}x\cos\tilde{n}y, \tag{65}$$

$$D_x=\sum_{\hat{m}=1}^{\infty}\sum_{\hat{n}=1}^{\infty}D_{x\hat{m}\hat{n}}(z)\cos\tilde{m}x\sin\tilde{n}y, \tag{66}$$

$$D_y=\sum_{\hat{m}=1}^{\infty}\sum_{\hat{n}=1}^{\infty}D_{y\hat{m}\hat{n}}(z)\sin\tilde{m}x\cos\tilde{n}y, \tag{67}$$

where

$$\begin{Bmatrix}\sigma_{x\hat{m}\hat{n}}\\ \sigma_{y\hat{m}\hat{n}}\\ \sigma_{xy\hat{m}\hat{n}}\end{Bmatrix}=\begin{bmatrix} l_{11}&l_{12}\\ l_{21}&l_{22}\\ l_{31}&l_{32}\end{bmatrix}\begin{Bmatrix}u_{\hat{m}\hat{n}}\\ v_{\hat{m}\hat{n}}\end{Bmatrix}+\begin{bmatrix}l_{13}\\ l_{23}\\ 0\end{bmatrix}\sigma_{z\hat{m}\hat{n}} + \begin{bmatrix}l_{14}\\ l_{24}\\ 0\end{bmatrix}D_{z\hat{m}\hat{n}},$$

$$\begin{Bmatrix}D_{x\hat{m}\hat{n}}\\ D_{y\hat{m}\hat{n}}\end{Bmatrix}=\begin{bmatrix} l_{41}&0\\ 0&l_{52}\end{bmatrix}\begin{Bmatrix}\sigma_{xz\hat{m}\hat{n}}\\ \sigma_{yz\hat{m}\hat{n}}\end{Bmatrix}+\begin{bmatrix}l_{43}\\ l_{53}\end{bmatrix}\phi_{\hat{m}\hat{n}},$$

and $l_{11} = -\tilde{m}\tilde{Q}_{11}$, $l_{12} = -\tilde{n}\tilde{Q}_{12}$, $l_{13} = a_1 h^2/L^2$, $l_{14} = b_1 e_0/Q$,

$$l_{21} = -\tilde{m}\tilde{Q}_{21}, \quad l_{12} = -\tilde{n}\tilde{Q}_{12}, \quad l_{23} = a_2 h^2/L^2,$$

$$l_{14} = b_1 e_0/Q, \quad l_{31} = \tilde{n}\tilde{Q}_{66}, \quad l_{32} = \tilde{m}\tilde{Q}_{66},$$
$$l_{41} = e_{15} Q h^2/e_0 c_{55} L^2,$$
$$l_{43} = -(c_{55}^{-1} e_{15}^2 + \eta_{11})(Qh^2/e_0^2 L^2)\tilde{m},$$
$$l_{52} = e_{24} Q h^2/e_0 c_{44} L^2,$$
$$l_{53} = -(c_{44}^{-1} e_{24}^2 + \eta_{22})(Qh^2/e_0^2 L^2)\tilde{n}.$$

Eq. (62) represents a system of eight simultaneously linear ordinary differential equations in terms of eight primary variables. A point collocation method based on the present DRKP approximations is applied to determine the primary variables in the elastic and electric fields. Once these primary variables are determined, the dependent variables can then be calculated using Eqs. (6)-(16).

6 Illustrative Examples

6.1 Single-layer homogeneous piezoelectric plates

The present DRKP method is applied to the coupled electro-elastic analysis of a single-layered piezoelectric plate. Selecting NP nodal points along the thickness coordinate from bottom to top surfaces of the plate with a uniform spacing and applying the present DRK approximations to Eq. (62) at each nodal point, we obtain

$$\left(\sum_{l=1}^{NP} \phi_l^{(1)}(z_k)\left(\hat{F}_i\right)_l\right) - \tilde{d}_{ij}\left(\sum_{l=1}^{NP} \phi_l(z_k)\left(\hat{F}_j\right)_l\right) = 0$$
$$\text{for } i = 1,2,3,\cdots,8 \text{ and } k = 1,2,3,\cdots,NP, \tag{68}$$

where $\hat{\mathbf{F}} = \left\{\hat{u} \quad \hat{v} \quad \hat{\sigma}_z \quad \hat{D}_z \quad \hat{\sigma}_{xz} \quad \hat{\sigma}_{yz} \quad \hat{w} \quad \hat{\phi}\right\}^T$ and $\left(\hat{F}_j\right)_l$ denotes the fictitious nodal value of j^{th} primary variable in $\hat{\mathbf{F}}$ at the l^{th} nodal point; z_k denotes the thickness coordinate of k^{th} referred nodal point.

Similarly, the DRK approximations for the boundary conditions on the lateral surfaces are given by

$$\begin{aligned} &\sum_{l=1}^{NP} \phi_l(z=-1)\left(\hat{F}_5\right)_l = 0, \\ &\sum_{l=1}^{NP} \phi_l(z=-1)\left(\hat{F}_6\right)_l = 0, \\ &\sum_{l=1}^{NP} \phi_l(z=-1)\left(\hat{F}_3\right)_l = \tilde{q}_0^-, \\ &\text{either } \sum_{l=1}^{NP} \phi_l(z=-1)\left(\hat{F}_8\right)_l = \tilde{\Phi}_0^- \\ &\text{or } \sum_{l=1}^{NP} \phi_l(z=-1)\left(\hat{F}_4\right)_l = \tilde{D}_0^-; \end{aligned} \tag{69}$$

$$\begin{aligned} &\sum_{l=1}^{NP} \phi_l(z=1)\left(\hat{F}_5\right)_l = 0, \\ &\sum_{l=1}^{NP} \phi_l(z=1)\left(\hat{F}_6\right)_l = 0, \\ &\sum_{l=1}^{NP} \phi_l(z=1)\left(\hat{F}_3\right)_l = \tilde{q}_0^+, \\ &\text{either } \sum_{l=1}^{NP} \phi_l(z=1)\left(\hat{F}_8\right)_l = \tilde{\Phi}_0^+ \\ &\text{or } \sum_{l=1}^{NP} \phi_l(z=1)\left(\hat{F}_4\right)_l = \tilde{D}_0^+; \end{aligned} \tag{70}$$

where $\tilde{q}_0^{\pm} = q_0^{\pm} L^3/(h^3 Q)$, $\tilde{\Phi}_0^{\pm} = Le\Phi_0^{\pm}/(h^2 Q)$ and $\tilde{D}_0^{\pm} = L\overline{D}_3^{\pm}/(he)$.

Equations (68)-(70) represent a linear mathematical system consisting of [(8×NP)+8] simultaneously algebraic equations in terms of (8xNP) unknowns. A weighted least square method is used in the present analysis where the weight number for the lateral boundary conditions is taken to be 10000 and for Euler-Lagrange equations is 1.

Table 2 considers a simply supported, single-layer homogeneous piezoelectric plate under the cylindrical bending type of electric potential. The applied electric potentials on lateral surfaces are given as $\overline{\Phi}^+(x_1) = \Phi_0 \sin(\pi x_1/L_1)$ and $\overline{\Phi}^-(x_1) = 0$. The material properties are given in Table 1 (Dube et al., 1996). The geometric parameter of S ($S = L_1/(2h)$) is taken as 4. For the comparison

Table 1: Elastic, piezoelectric and dielectric properties of piezoelectric materials

Moduli	Crystal class mm2 (Dube et al., 1996)	Ceramics (Heyliger and Brooks, 1996)	PZT-4 (Heyliger and Brooks, 1996)	Moduli	PZT-4 (Heyliger, 1994)	Composite Material (Heyliger, 1994)
c_{11} (GPa)	74.1	138.28	139.02	E_{11} (GPa)	81.3	132.38
c_{22}	74.1	138.28	139.02	E_{22}	81.3	10.756
c_{33}	82.6	128.07	115.45	E_{33}	64.5	10.756
c_{12}	45.2	32.359	77.848	v_{12}	0.329	0.24
c_{23}	39.3	27.821	74.328	v_{13}	0.432	0.24
c_{13}	39.3	27.821	74.328	v_{23}	0.432	0.49
c_{44}	13.17	53.5	25.6	G_{44}	25.6	3.606
c_{55}	13.17	53.5	25.6	G_{55}	25.6	5.654
c_{66}	14.45	53.0	30.6	G_{66}	30.6	5.654
e_{24} (C/m^2)	0.0	2.96	12.72	e_{24} (C/m^2)	12.72	0.000
e_{15}	-0.138	2.96	12.72	e_{15}	12.72	0.000
e_{31}	-0.160	0.8	-5.2	e_{31}	-5.20	0.000
e_{32}	-0.160	0.8	-5.2	e_{32}	-5.20	0.000
e_{33}	0.347	6.88	15.08	e_{33}	15.08	0.000
η_{11} (F/m)	0.825e-10	1.7885e-09	1.306e-08	η_{11} (F/m)	1.306e-08	0.3099e-10
η_{22}	0.825e-10	1.7885e-09	1.306e-08	η_{22}	1.306e-08	0.2656e-10
η_{33}	0.902e-10	1.6026e-09	1.151e-08	η_{33}	1.151e-08	0.2656e-10

purpose, a set of normalized field variables used by Dube et al. (1996) is adopted and given by

$$\tilde{u} = 100u/\left(S|d_1|\Phi_0\right), \quad \tilde{w} = 100w/\left(|d_1|\Phi_0\right),$$

$$\tilde{\sigma}_x = S^2(2h)\sigma_x/\left(Y_x|d_1|\Phi_0\right),$$

$$\tilde{\sigma}_y = (2h)\sigma_y/\left(Y_x|d_1|\Phi_0\right),$$

$$\tilde{\sigma}_z = S^4(2h)\sigma_z/\left(Y_x|d_1|\Phi_0\right),$$

$$\tilde{\sigma}_{xz} = S^3(2h)\sigma_{xz}/\left(Y_x|d_1|\Phi_0\right),$$

$$\tilde{\phi} = \Phi/\Phi_0, \quad \tilde{D}_z = (2h)D_z/\left(Y_x d_1^2\Phi_0\right),$$

$$d_1 = -3.9238x10^{-12}\,\text{C/N}, \quad Y_x = 42.785\,\text{GPa}. \tag{71}$$

Table 2 shows the present solutions of various variables of elastic and electric fields at the crucial positions in the piezoelectric plate where a uniform spacing (Δx_3) for each pair of neighboring nodal points is used. The number of total nodal points is taken as NP=5, 7, 9, 11, 21 and $\Delta x_3 = 2h/(NP-1)$. The effects of the highest order of basis functions (n) and the support size (a) on the present solutions are presented where the values of (n, Δx_3) are taken as (2, 2.1Δx_3), (2, 3.1Δx_3) and (3, 3.1Δx_3). The accuracy and rate of convergence of the present DRKP method are validated by comparing the present solutions with the available 3D solutions in the literature (Dube et al., 1996). It is shown that the present solutions with n=3 and a=3.1Δx_3 yield more accurate results than the others. It is shown that the present solutions rapidly converge and the present 11-nodes solutions are in excellent agreement with the available 3D solutions.

Table 2: The elastic and electric field variables in a single-layer piezoelectric plate under electric potential ($S = 4$)

n	a	Theories	$\tilde{u}(0,-h)$	$\tilde{w}\left(\frac{a}{2},0\right)$	$\tilde{\sigma}_x\left(\frac{a}{2},h\right)$	$\tilde{\sigma}_y\left(\frac{a}{2},h\right)$	$\tilde{\sigma}_z\left(\frac{a}{2},0\right)$	$\tilde{\sigma}_{xz}\left(0,-\frac{h}{2}\right)$	$\bar{\phi}\left(\frac{a}{2},0\right)$	$\tilde{D}_z\left(\frac{a}{2},h\right)$
2	$2.1\,\Delta x_3$	$NP = 5$	-32.6646	186.9630	-7.0673	-1.3960	4.3240	2.7420	0.4631	-167.4022
		7	-33.9453	191.7344	-6.4980	-1.3786	1.7834	1.7581	0.4679	-167.4153
		9	-34.1341	189.5465	-6.3403	-1.3733	2.1483	1.6563	0.4670	-167.3555
		11	-34.1889	190.6273	-6.2747	-1.3711	1.8513	1.7171	0.4674	-167.3171
		21	-34.2495	190.5475	-6.1941	-1.3681	1.8525	1.7215	0.4673	-167.2543
2	$3.1\,\Delta x_3$	$NP = 5$	-32.1716	188.7672	-7.5277	-1.4141	4.4815	2.4717	0.4666	-167.9715
		7	-33.9405	189.5640	-6.7097	-1.3870	2.2375	1.7174	0.4676	-167.6904
		9	-34.0600	189.2202	-6.4724	-1.3785	2.2406	1.7229	0.4674	-167.5167
		11	-34.1228	189.9439	-6.3696	-1.3747	2.0232	1.7246	0.4674	-167.4233
		21	-34.2278	190.4670	-6.2228	-1.3692	1.8798	1.7168	0.4673	-167.2827
3	$3.1\,\Delta x_3$	$NP = 5$	-33.9632	190.4563	-6.2248	-1.3688	1.7765	1.7940	0.4671	-167.2162
		7	-34.2586	190.8505	-6.1789	-1.3675	1.7767	1.7161	0.4673	-167.2276
		9	-34.2697	190.6588	-6.1701	-1.3672	1.8041	1.7181	0.4673	-167.2289
		11	-34.2702	190.6878	-6.1682	-1.3672	1.8067	1.7191	0.4673	-167.2293
		21	-34.2698	190.6816	-6.1674	-1.3672	1.8110	1.7190	0.4673	-167.2294
		Exact solution (Dube et al.,1996)	-34.27	190.7	-6.167	-1.367	1.811	1.719	0.4673	-167.2

$\Delta x_3 = 2h/(NP-1)$

Table 3: The elastic and electric field variables in a two-layer piezoelectric plate under cylindrical bending type of mechanical load

ζ	Theories	$\bar{v}(0,\zeta)\times10^{13}$	$\bar{w}\left(\frac{L}{2},\zeta\right)\times10^{10}$	$\bar{\phi}\left(\frac{L}{2},\zeta\right)\times10^{4}$	$\bar{\sigma}_y\left(\frac{L}{2},\zeta\right)$	$\bar{\tau}_{yz}(0,\zeta)$	$\bar{\sigma}_z\left(\frac{L}{2},\zeta\right)$	$\bar{D}_z\left(\frac{L}{2},\zeta\right)\times10^{10}$
h	DRKP NP=7	-170.374	1.05566	0.00000	57.8768	0.00000	1.000000	-2.21441
	9	-170.416	1.05613	0.00000	57.8908	0.00000	1.000000	-2.21653
	11	-170.415	1.05612	0.00000	57.8904	0.00000	1.000000	-2.21645
	21	-170.415	1.05613	0.00000	57.8905	0.00000	1.000000	-2.21653
	Wu et al. (2007)	-170.415	1.05613	0.00000	57.8904	0.00000	1.000000	-2.21653
	Heyliger and Brooks (1996)	-170.406	1.05609	0.00000	57.8914	0.00000	1.000000	-2.21625
0.5h	DRKP NP=7	-88.8697	1.06070	10.5730	30.1851	3.45515	0.850178	-2.67778
	9	-88.8866	1.06109	10.5727	30.1905	3.45484	0.850105	-2.68014
	11	-88.8859	1.06108	10.5728	30.1903	3.45474	0.850100	-2.68007
	21	-88.8862	1.06109	10.5729	30.1903	3.45473	0.850098	-2.68015
	Wu et al. (2007)	-88.8861	1.06109	10.5729	30.1903	3.45473	0.850098	-2.68015
	Heyliger and Brooks (1996)	-88.8804	1.06105	10.5763	30.1904	3.45477	0.850095	-2.67988
0	DRKP NP=7	-9.13372	1.06256	14.0608	2.93287	4.75307	0.513743	-3.73228
	9	-9.13413	1.06296	14.0663	2.93278 (3.77200)	4.75390	0.513739	-3.73430
	11	-9.13406	1.06295	14.0661	2.93277 (3.77198)	4.75387	0.513739	-3.73420
	21	-9.13403	1.06295	14.0663	2.93275 (3.77196)	4.75387	0.513739	-3.73427
	Wu et al. (2007)	-9.13402	1.06295	14.0662	2.93275 (3.77196)	4.75387	0.513739	-3.73427
	Heyliger and Brooks (1996)	-9.13120	1.06291	14.0706	2.93185 (3.77076)	4.75387	0.513734	-3.73402
-0.5h	DRKP NP=7	72.3010	1.06228	8.14234	-30.1957	3.71761	0.163562	-3.87166
	9	72.3133	1.06267	8.14385	-30.2008	3.71722	0.163619	-3.87363
	11	72.3127	1.06267	8.14363	-30.2006	3.71711	0.163623	-3.87354
	21	72.3129	1.06267	8.14371	-30.2007	3.71710	0.163625	-3.87361
	Wu et al. (2007)	72.3128	1.06267	8.14370	-30.2007	3.71709	0.163625	-3.87361
	Heyliger and Brooks (1996)	72.3126	1.06263	8.14620	-30.2007	3.71705	0.163623	-3.87336
-h	DRKP NP=7	150.735	1.06069	0.00000	-64.5397	0.00000	0.000000	-3.94165
	9	154.770	1.06116	0.00000	-64.5542	0.00000	0.000000	-3.94364
	11	154.769	1.06115	0.00000	-64.5538	0.00000	0.000000	-3.94355
	21	154.769	1.06116	0.00000	-64.5538	0.00000	0.000000	-3.94362
	Wu et al. (2007)	154.769	1.06116	0.00000	-64.5538	0.00000	0.000000	-3.94362
	Heyliger and Brooks (1996)	154.765	1.06112	0.00000	-64.5526	0.00000	0.000000	-3.94337

6.2 Multilayered elastic and piezoelectric plates

The present DRKP method is also applied to the coupled electro-elastic analysis of multilayered elastic and piezoelectric plates. Selecting $NP^{(m)}$ nodal points along the thickness coordinate from bottom to top surfaces of the m^{th}-layer and applying the present DRK approximations to Eq. (62) at each nodal point, we obtain

$$\left(\sum_{l=1}^{NP}\phi_l^{(1)}(z_k^{(m)})\left(\hat{F}_i^{(m)}\right)_l\right) - \tilde{d}_{ij}^{(m)}\left(\sum_{l=1}^{NP}\phi_l(z_k^{(m)})\left(\hat{F}_j^{(m)}\right)_l\right) = 0$$

for $i = 1,2,3,\cdots,8$ and $k = 1,2,3,\cdots,NP^{(m)}$, (72)

where

Table 4: The elastic and electric field variables in a two-layer piezoelectric plate under cylindrical bending type of electric potential

ζ	Theories	$\bar{v}(0,\zeta)\times10^{11}$	$\bar{w}\left(\frac{L}{2},\zeta\right)\times10^{10}$	$\bar{\phi}\left(\frac{L}{2},\zeta\right)$	$\bar{\sigma}_y\left(\frac{L}{2},\zeta\right)$	$\bar{\tau}_{yz}(0,\zeta)$	$\bar{\sigma}_z\left(\frac{L}{2},\zeta\right)\times10^2$	$\bar{D}_z\left(\frac{L}{2},\zeta\right)\times10^7$
h	DRKP *NP*=7	-17.2271	2.21492	1.000000	98.0248	0.00000	0.00000	-4.38166
	9	-17.2285	2.21654	1.000000	98.0680	0.00000	0.00000	-4.38171
	11	-17.2285	2.21650	1.000000	98.0664	0.00000	0.00000	-4.38171
	21	-17.2285	2.21653	1.000000	98.0665	0.00000	0.00000	-4.38171
	Wu et al. (2007)	-17.2285	2.21653	1.000000	98.0664	0.00000	0.00000	-4.38171
	Heyliger and Brooks (1996)	-17.2277	2.21625	1.000000	98.0706	0.00000	0.00000	-4.38016
$0.5h$	DRKP NP=7	-11.6674	2.37228	0.935603	-39.0097	2.31359	-16.1184	-3.91981
	9	-11.6682	2.37367	0.935608	-38.9875	2.31079	-16.1146	-3.91986
	11	-11.6682	2.37361	0.935608	-38.9882	2.31032	-16.1155	-3.91986
	21	-11.6682	2.37365	0.935609	-38.9881	2.31026	-16.1156	-3.91987
	Wu et al. (2007)	-11.6682	2.37365	0.935608	-38.9881	2.31023	-16.1157	-3.91986
	Heyliger and Brooks (1996)	-11.6676	2.37336	0.935611	-38.9872	2.31044	-16.1166	-3.91847
0	DRKP NP=7	-6.21149	2.49685	0.874721	-175.595 (135.711)	-6.11577	-8.21644	-3.48672
	9	-6.21174	2.49839	0.874731	-175.591 (135.720)	-6.11231	-8.20430	-3.48676
	11	-6.21173	2.49835	0.874731	-175.591 (135.720)	-6.11243	-8.20483	-3.48676
	21	-6.22174	2.49838	0.874732	-175.591 (135.720)	-6.11242	-8.20464	-3.48676
	Wu et al. (2007)	-6.21174	2.49838	0.874731	-175.591 (135.720)	-6.11243	-8.20466	-3.48676
	Heyliger and Brooks (1996)	-6.21137	2.49809	0.874736	-175.593 (135.710)	-6.11227	-8.20718	-3.48550
$-0.5h$	DRKP NP=7	-3.85943	2.74103	0.436351	38.9647	0.744316	7.90082	-3.45506
	9	-3.85895	2.74248	0.436357	38.9429	0.744193	7.90383	-3.44465
	11	-3.85896	2.74242	0.436357	38.9437	0.743848	7.90396	-3.45511
	21	-3.85896	2.74246	0.436357	38.9436	0.743840	7.90413	-3.45511
	Wu et al. (2007)	-3.85896	2.74246	0.436357	38.9437	0.743825	7.90414	-3.45511
	Heyliger and Brooks (1996)	-3.85882	2.74217	0.436359	38.9426	0.743546	7.90257	-3.45386
$-h$	DRKP NP=7	-1.52206	2.97988	0.00000	-57.9642	0.00000	0.00000	-3.44460
	9	-1.52079	2.98147	0.00000	-58.0187	0.00000	0.00000	-3.44465
	11	-1.52083	2.98143	0.00000	-58.0169	0.00000	0.00000	-3.44464
	21	-1.52082	2.98146	0.00000	-58.0172	0.00000	0.00000	-3.44465
	Wu et al. (2007)	-1.52083	2.98145	0.00000	-58.0171	0.00000	0.00000	-3.44464
	Heyliger and Brooks (1996)	-1.52091	2.98116	0.00000	-58.0090	0.00000	0.00000	-3.44340

$$\hat{\mathbf{F}}^{(m)} = \left\{ \hat{u}^{(m)} \quad \hat{v}^{(m)} \quad \hat{\sigma}_z^{(m)} \quad \hat{D}_z^{(m)} \quad \hat{\sigma}_{xz}^{(m)} \quad \hat{\sigma}_{yz}^{(m)} \quad \hat{w}^{(m)} \quad \hat{\phi}^{(m)} \right\}^T$$

and $\left(\hat{F}_j^{(m)}\right)_l$ denotes the fictitious nodal value of j^{th} primary variable in $\hat{\mathbf{F}}^{(m)}$ at the l^{th} nodal point of the m^{th}-layer. In the present analysis, we let $NP^{(m)} = NP$ and $\Delta x_3^{(m)} = 2h^{(m)}/(NP-1)$, $m = 1,2,3\cdots,NL$ where $2h^{(m)}$ denotes the thickness of the m^{th}-layer and $2h^{(m)} = z_{NP}^{(m)} - z_1^{(m)}$.

Similarly, the DRK approximations for the boundary conditions on the lateral surfaces are

Table 5: The elastic and electric field variables in a two-layer piezoelectric plate under cylindrical bending type of electric displacement

ζ	Theories	$\bar{v}(0,\zeta)\times 10^{6}$	$\bar{w}\left(\frac{L}{2},\zeta\right)\times 10^{3}$	$\bar{\phi}\left(\frac{L}{2},\zeta\right)\times 10^{-6}$	$\bar{\sigma}_{y}\left(\frac{L}{2},\zeta\right)\times 10^{-6}$	$\bar{\tau}_{yz}(0,\zeta)\times 10^{-5}$	$\bar{\sigma}_{z}\left(\frac{L}{2},\zeta\right)\times 10^{-5}$	$\bar{D}_{z}\left(\frac{L}{2},\zeta\right)$
h	DRKP NP=7	429.0613	1.54993	-9.62434	-345.1262	0.0000	0.00000	1.0000000
	9	429.0517	1.54985	-9.62432	-345.0937	0.0000	0.00000	1.0000000
	11	429.0516	1.54985	-9.62432	-345.0934	0.0000	0.00000	1.0000000
	21	429.0510	1.54985	-9.62432	-345.0915	0.0000	0.00000	1.0000000
	Wu et al. (2007)	429.0510	1.54985	-9.62432	-345.0915	0.0000	0.00000	1.0000000
$0.5h$	DRKP NP=7	177.2110	1.51923	-9.50763	1.7511	-134.7230	7.07033	0.5431662
	9	177.2146	1.51928	-9.50763	1.7404	-134.5574	7.06543	0.5431676
	11	177.2144	1.51929	-9.50763	1.7411	-134.5459	7.06580	0.5431676
	21	177.2145	1.51929	-9.50763	1.7408	-134.5430	7.06579	0.5431677
	Wu et al. (2007)	177.2145	1.51929	-9.50763	1.7408	-134.5425	7.06581	0.5431676
0	DRKP NP=7	-72.9028	1.50961	-9.45347	347.2639 (335.5428)	2.3898	14.04560	0.0904129
	9	-72.8846	1.50955	-9.45347	347.2014 (335.4665)	2.3745	14.03095	0.0904129
	11	-72.8890	1.50955	-9.45347	347.2025 (335.4679)	2.3754	14.03141	0.0904129
	21	-72.8842	1.50955	-9.45347	347.2002 (335.4650)	2.3752	14.03126	0.0904129
	Wu et al. (2007)	-72.8842	1.50955	-9.45347	347.2001 (335.4649)	2.3752	14.03128	0.0904129
$-0.5h$	DRKP NP=7	4.2154	1.50556	-9.36675	-1.5336	133.5282	6.97584	0.0450689
	9	4.2130	1.50546	-9.36677	-1.5239	133.3767	6.96867	0.0450689
	11	4.2131	1.50545	-9.36677	-1.5245	133.3693	6.96888	0.0450689
	21	4.2131	1.50546	-9.36677	-1.5243	133.3671	6.96881	0.0450689
	Wu et al. (2007)	4.2131	1.50545	-9.36676	-1.5244	133.3667	6.96882	0.0450689
$-h$	DRKP NP=7	81.3398	1.50331	-9.33942	-338.5371	0.0000	0.00000	0.0000000
	9	81.3166	1.50325	-9.33942	-338.4408	0.0000	0.00000	0.0000000
	11	81.3172	1.50325	-9.33942	-338.4434	0.0000	0.00000	0.0000000
	21	81.3165	1.50325	-9.33942	-338.4402	0.0000	0.00000	0.0000000
	Wu et al. (2007)	81.3164	1.50325	-9.33942	-338.4401	0.0000	0.00000	0.0000000

given by

$$\sum_{l=1}^{NP}\phi_l(z=-1)\left(\hat{F}_5^{(1)}\right)_l=0,$$
$$\sum_{l=1}^{NP}\phi_l(z=-1)\left(\hat{F}_6^{(1)}\right)_l=0,$$
$$\sum_{l=1}^{NP}\phi_l(z=-1)\left(\hat{F}_3^{(1)}\right)_l=\tilde{q}_0^{-}, \tag{73}$$
$$\text{either }\sum_{l=1}^{NP}\phi_l(z=-1)\left(\hat{F}_8^{(1)}\right)_l=\tilde{\Phi}_0^{-}$$
$$\text{or }\sum_{l=1}^{NP}\phi_l(z=-1)\left(\hat{F}_4^{(1)}\right)_l=\tilde{D}_0^{-};$$

$$\sum_{l=1}^{NP}\phi_l(z=1)\left(\hat{F}_5^{(NL)}\right)_l=0,$$
$$\sum_{l=1}^{NP}\phi_l(z=1)\left(\hat{F}_6^{(NL)}\right)_l=0,$$
$$\sum_{l=1}^{NP}\phi_l(z=1)\left(\hat{F}_3^{(NL)}\right)_l=\tilde{q}_0^{+}, \tag{74}$$
$$\text{either }\sum_{l=1}^{NP}\phi_l(z=1)\left(\hat{F}_8^{(NL)}\right)_l=\tilde{\Phi}_0^{+}$$
$$\text{or }\sum_{l=1}^{NP}\phi_l(z=1)\left(\hat{F}_4^{(NL)}\right)_l=\tilde{D}_0^{+}.$$

The DRK approximations for the continuity conditions at interfaces between adjacent layers are also given by

$$\sum_{l=1}^{NP} \phi_l(z=z_{NP}^{(m)}) \left(\hat{F}_i^{(m)}\right)_l = \sum_{l=1}^{NP} \phi_l(z=z_1^{(m+1)}) \left(\hat{F}_i^{(m+1)}\right)_l$$
$$\text{for } i=1,2,3,\cdots,8 \text{ and } m=1,2,\cdots,(NL-1). \tag{75}$$

Equations (72)-(75) represent a linear mathematical system consisting of [(8×NP×NL)+(8xNL)] simultaneously algebraic equations in terms of (8×NP×NL) unknowns. Again, the weighted least square method is used in the present analysis where the weight number for both the lateral boundary conditions and continuity conditions is taken to be 10000 and for Euler-Lagrange equations is 1.

Tables 3-5 consider a simply supported, two-layered laminate composed of [PZT-4/ceramics] with equal thickness layers under the cylindrical bending type of mechanical load, electric potential and electric displacement, respectively. The applied mechanical load, electric potential and electric displacement on lateral surfaces are given as $\overline{q}_3^+(x_2) = q_0\sin(\pi x_2/L_2)$, $\overline{q}_3^-(x_2) = 0$; $\overline{\Phi}^+(x_2) = \Phi_0\sin(\pi x_2/L_2)$, $\overline{\Phi}^-(x_2) = 0$; $\overline{D}_3^+(x_2) = D_0\sin(\pi x_2/L_2)$, $\overline{D}_3^-(x_2) = 0$ for Tables 3-5, respectively. The material properties of PZT-4 and ceramics layers are given in Table 1 (Heyliger and Brooks, 1996). The dimensions of length and total thickness of the plate are L_2=0.1m and $2h$=0.01m. Tables 3-5 show the present DRKP solutions of elastic and electric field components at the middle surface of each layer and at the interface between the dissimilar layers where the values of (n, a) are taken as (3, $3.1\Delta x_3^{(m)}$) for each layer. The present DRKP solutions are compared with the 3D solutions obtained from both Heyliger and Brooks (1996) using Pagano's approach (1969, 1970) and Wu et al. (2007) using an asymptotic approach. It is shown that the present solutions rapidly converge and the present solutions with 11 nodes at each layer are in excellent agreement with both available 3D solutions.

A multilayered piezoelectric plate composed of [0°/90°/0°] laminated composite plate bounded with piezoelectric layers (PZT-4) on the outer surfaces under mechanical load, piezoelectric potential and piezoelectric displacement is considered in Figures 2-4, respectively. The applied mechanical load, electric potential and electric displacement on lateral surfaces are given as $\overline{q}_3^+ = q_0\sin(\pi x_1/L_1)\sin(\pi x_2/L_2)$, $\overline{q}_3^- = 0$; $\overline{\Phi}^+ = \Phi_0\sin(\pi x_1/L_1)\sin(\pi x_2/L_2)$, $\overline{\Phi}^- = 0$; $\overline{D}_3^+ = D_0\sin(\pi x_1/L_1)\sin(\pi x_2/L_2)$, $\overline{D}_3^- = 0$ for Figures 2-4, respectively. The material properties of PZT-4 and composite layers are given in Table 1 (Heyliger, 1994). The dimensions of length and total thickness of the plate are $L_1 = L_2 = L$ and $L/2h = 4, 10, 20$. The thickness ratio of each layer is PZT-4 layer: 0°-layer: 90°-layer: 0°-layer: PZT-4 layer=0.1h: 0.6h: 0.6h: 0.6h: 0.1h. A set of normalized elastic and electric variables are given as follows:

For the applied mechanical load cases,

$$\begin{aligned}
&(\overline{u},\overline{w}) = (u_1,u_3)c^*/q_0(2h),\\
&(\overline{\tau}_{xz},\overline{\sigma}_z) = (\sigma_{13},\sigma_3)/q_0,\\
&\overline{\phi} = \Phi e^*/q_0(2h),\\
&\overline{D}_z = D_3c^*/(q_0e^*);
\end{aligned} \tag{76}$$

For the applied electric potential cases,

$$\begin{aligned}
&(\overline{u},\overline{w}) = (u_1,u_3)c^*/(\Phi_0e^*),\\
&(\overline{\tau}_{xz},\overline{\sigma}_z) = (\sigma_{13},\sigma_3)(2h)/(\Phi_0e^*),\\
&\overline{\phi} = \Phi/\Phi_0,\\
&\overline{D}_z = D_3c^*(2h)/\Phi_0(e^*)^2;
\end{aligned} \tag{77}$$

For the applied electric displacement cases,

$$\begin{aligned}
&(\overline{u},\overline{w}) = (u_1,u_3)e^*/(2hD_0),\\
&(\overline{\tau}_{xz},\overline{\sigma}_z) = (\sigma_{13},\sigma_3)e^*/(D_0c^*),\\
&\overline{\phi} = \Phi(e^*)^2/(2hD_0c^*),\\
&\overline{D}_z = D_3/D_0;
\end{aligned} \tag{78}$$

where $c^* = 1$ N/m^2, $e^* = 1$ C/m^2.

Figures 2-4 present the through-the-thickness distributions of various elastic and electric variables of the [PZT-4/0°/90°/0°/PZT-4] laminated plates under mechanical load, electric potential and electric displacement, respectively. It is shown that

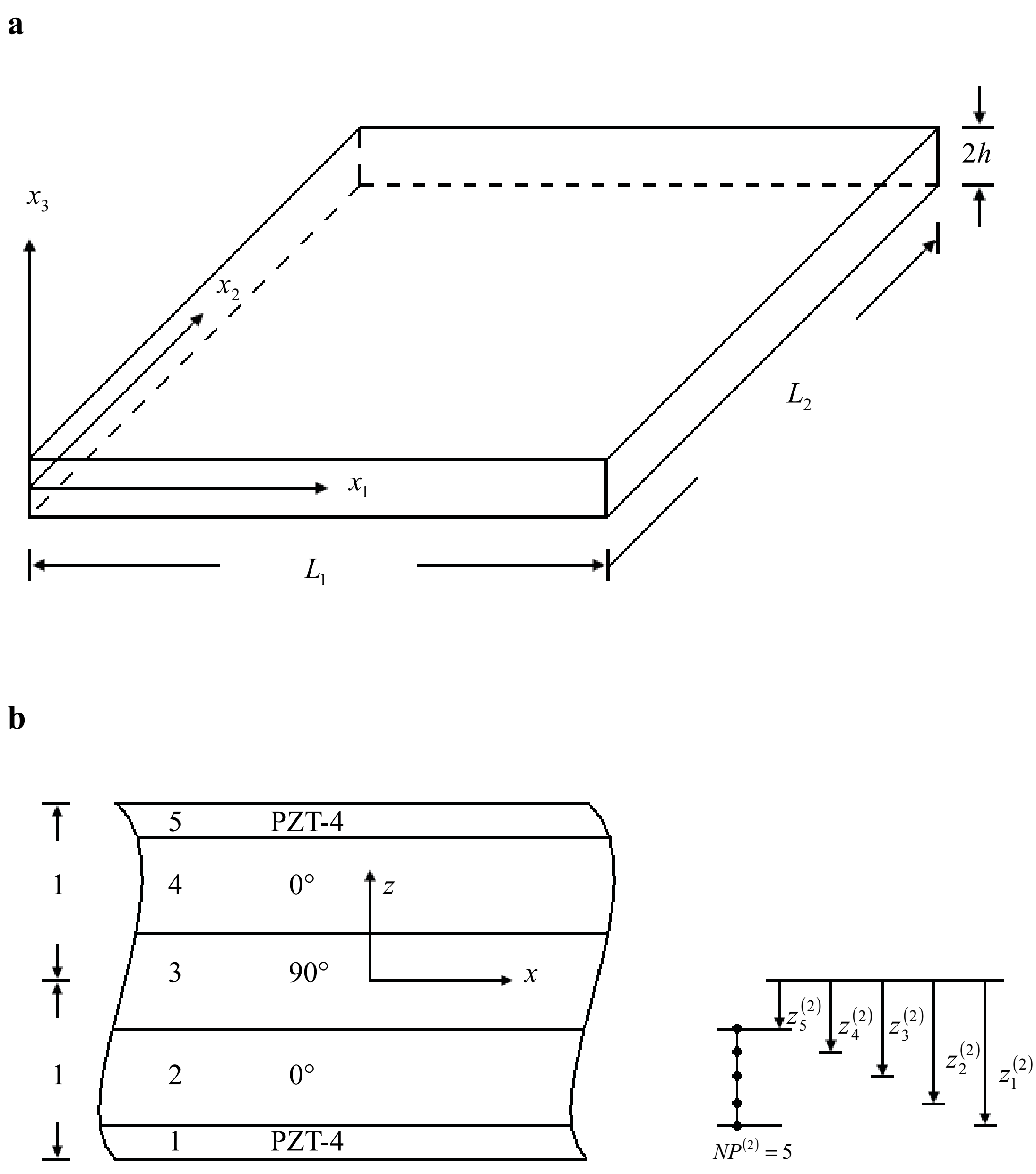

Figure 1: (a) The geometry and coordinates of a piezoelectric plate; (b) The dimensionless thickness coordinates of nodal points in a typical laminated [PZT-4/0°/90°/0°/PZT-4] plate.

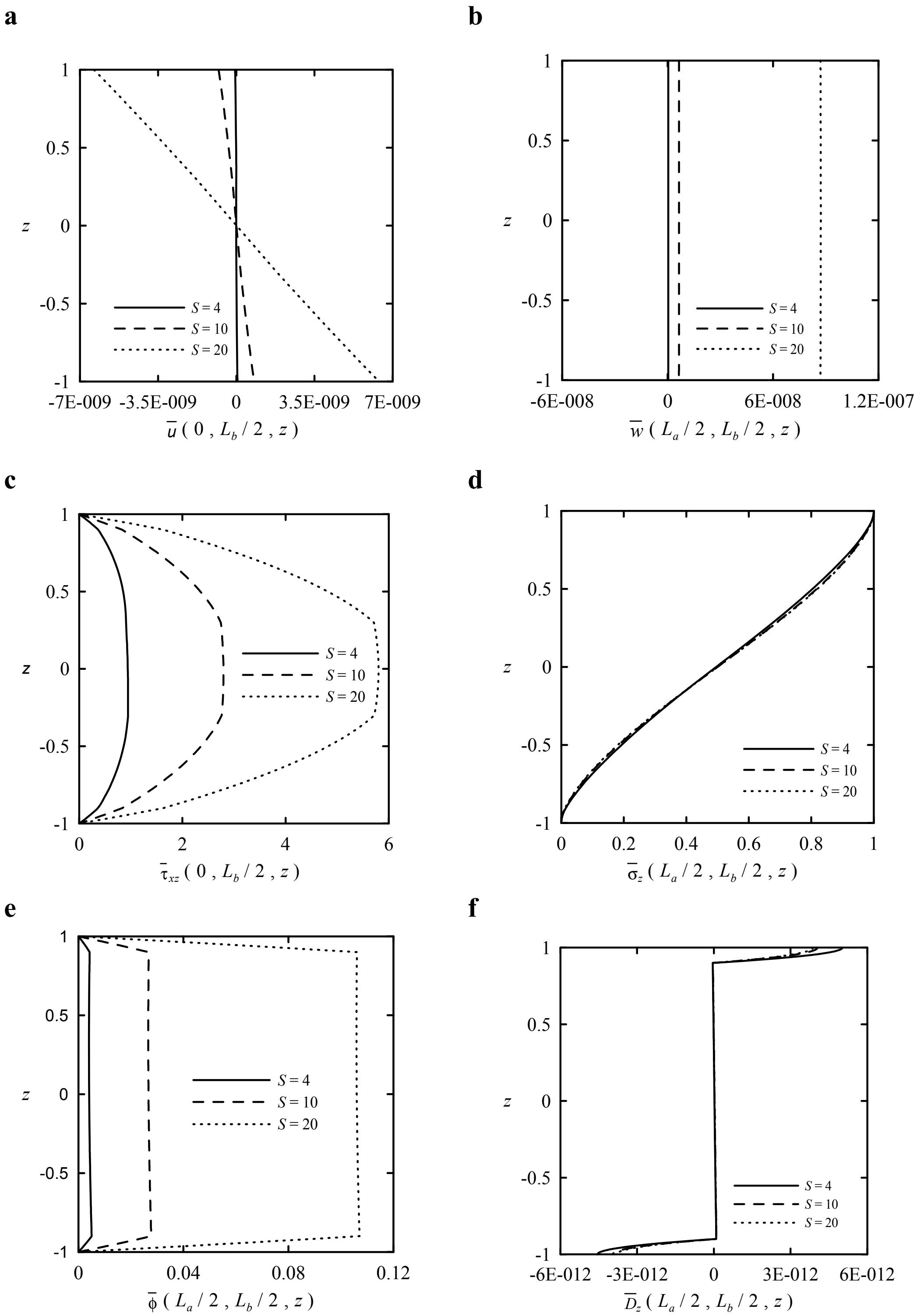

Figure 2: The through-the-thickness distributions of various field variables in a laminated [PZT-4/0°/90°/0°/PZT-4] plate under mechanical load.

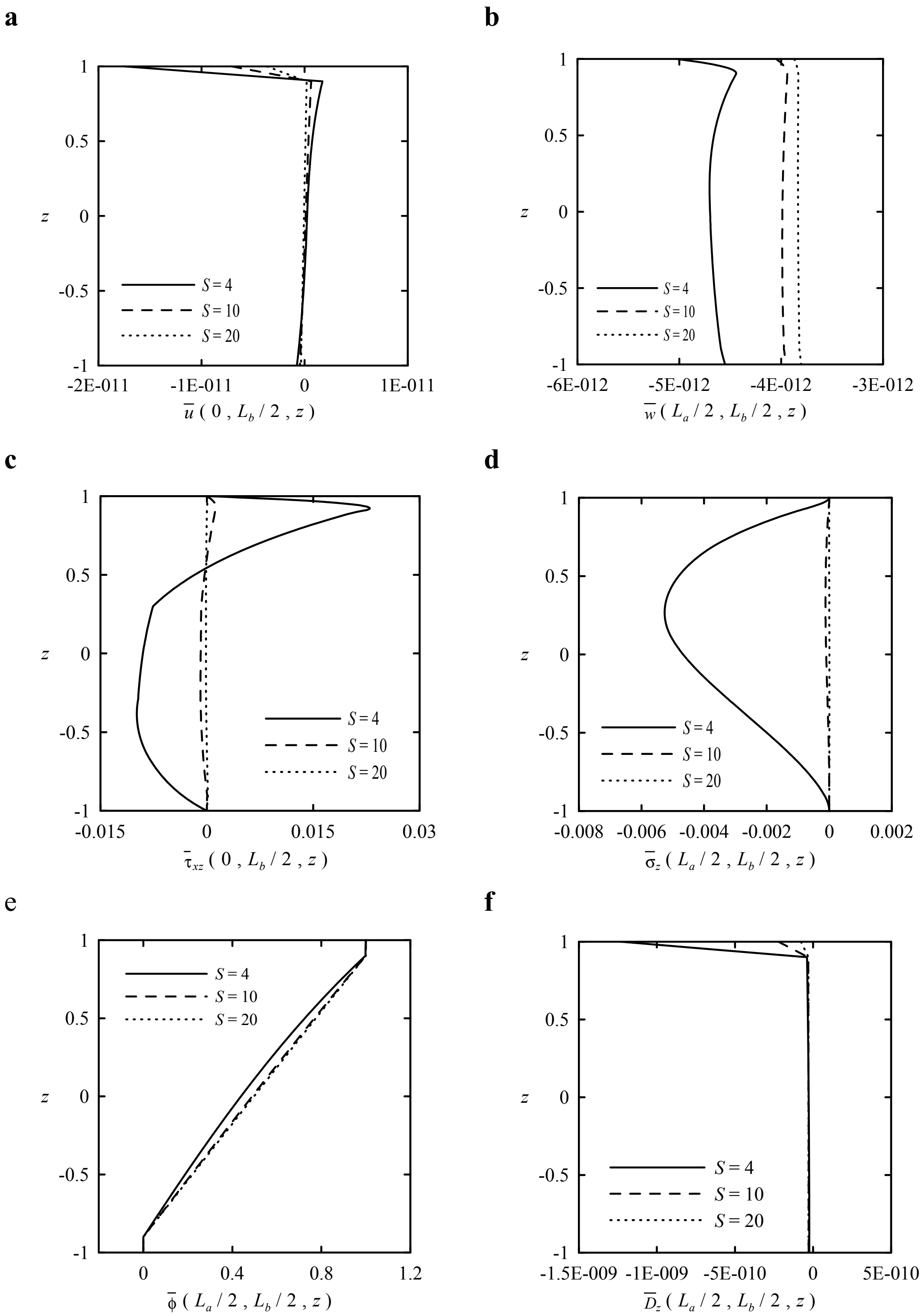

Figure 3: The through-the-thickness distributions of various field variables in a laminated [PZT-4/0°/90°/0°/PZT-4] plate under electric potential.

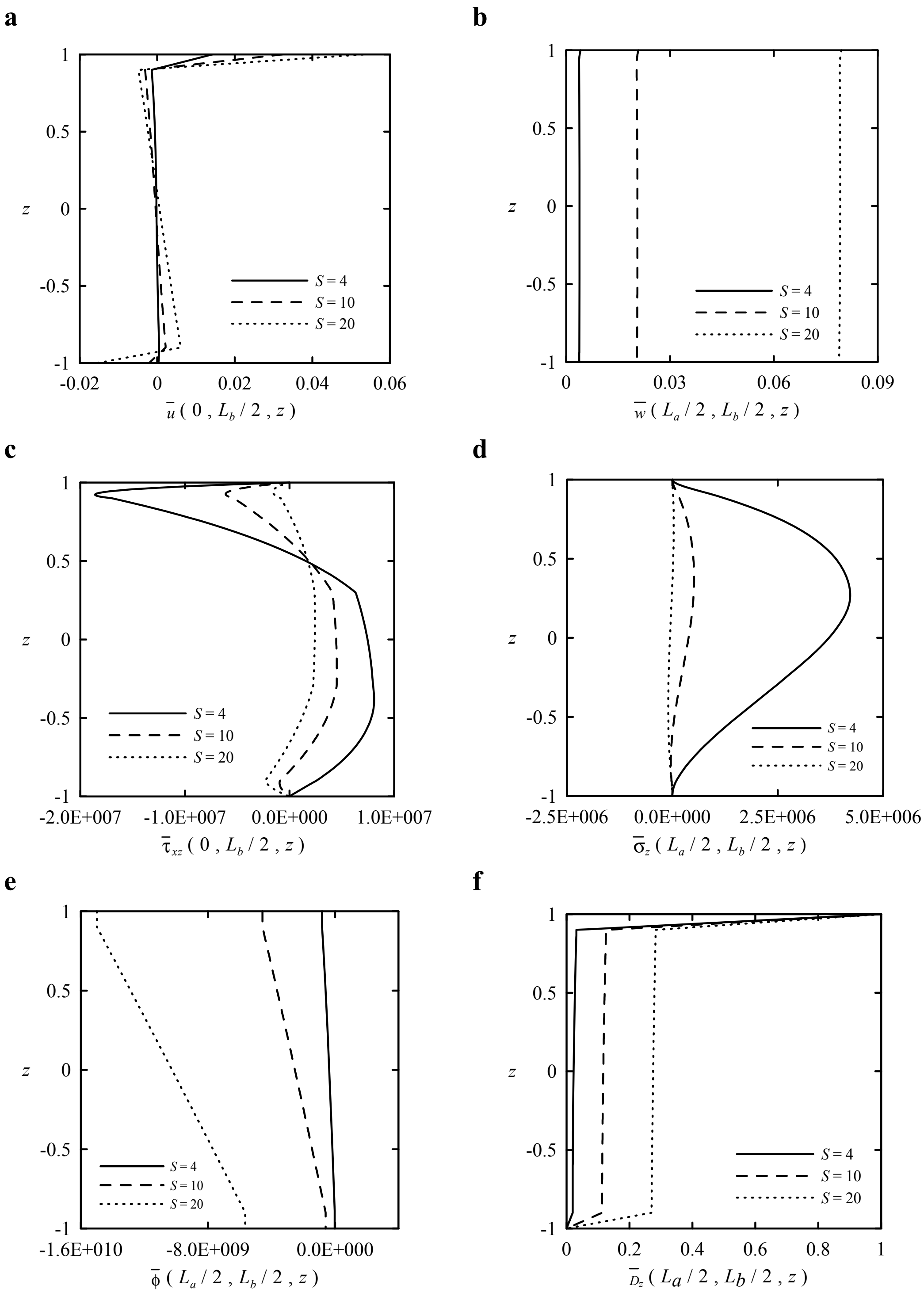

Figure 4: The through-the-thickness distributions of various field variables in a laminated [PZT-4/0°/90°/0°/PZT-4] plate under electric displacement.

the transverse shear stresses produced in the plate decrease as the plates become thicker for the applied mechanical load cases; contrarily, they increase as the plates become thicker for the applied electric load cases. The maximum transverse shear stresses occur in the composite material layer for the applied mechanical load cases; they, however, occur at interfaces between elastic and piezoelectric layers for the applied electric load cases. The distributions of the elastic displacements through the thickness coordinate are merely linear functions for the applied mechanical load cases; they, however, reveal approximately layerwise linear or higher-order polynomial functions for the applied electric load cases. It is observed that the through-the-thickness distributions of elastic and electric variables reveal large difference between the applied mechanical load cases and the applied electric load cases.

7 Conclusions

In this paper, we have proposed a differential reproducing kernel particle method for the analysis of multilayered piezoelectric plates. The newly proposed DRKP method is efficient for determinations of the shape functions of the derivatives of the reproducing kernel approximants using a set of differential reproducing conditions. The present DRKP method has been applied to the coupled elastic-electric analysis of multilayered piezoelectric plates under electromechanical loads. It is shown that the present DRKP solutions converge rapidly and are in excellent agreement with the available 3D solutions. In the present analysis, it is concluded that the basic kinematics assumptions of generalized 2D plate theories based on the global displacement fields, such as the classical plate theory, the first-order and higher-order shear deformation theories etc, may not be suitable for the analysis of multilayered piezoelectric plates under the electric load. Hence, an advanced 2D plate theory accounting for the layerwise nonlinear distributions of generalized kinematics variables in elastic and electric fields through the thickness coordinate is needed to be developed.

Acknowledgement: This work is supported by the National Science Council of Republic of China through Grant NSC 96-2221-E006-265.

References

Atluri, S.N. (2004): The Meshless Local Petrov-Galerkin (MLPG) Method for Domain & Boundary Discretizations, Tech Science Press, 700 pages, Forsyth, GA.

Atluri, S.N.; Cho, J.Y.; Kim, H.G. (1999): Analysis of thin beams, using the meshless local Petrov-Galerkin method, with generalized moving least squares interpolations. *Comput. Mech.*, vol. 24, pp. 334-347.

Atluri, S.N.; Han, Z.D.; Rajendran, A.M. (2004): A new implementation of the meshless finite volume method through the MLPG mixed approach. *CMES: Computer Modeling in Engineering & Sciences*, vol. 6, pp. 419-514.

Atluri, S.N.; Liu, H.T.; Han, Z.D. (2006a): Meshless local Petrov-Galerkin (MLPG) mixed collocation method for elasticity problems. *CMES: Computer Modeling in Engineering & Sciences*, vol. 14, pp. 141-152.

Atluri, S.N.; Liu, H.T.; Han, Z.D. (2006b): Meshless local Petrov-Galerkin (MLPG) mixed finite difference method for solid mechanics. *CMES: Computer Modeling in Engineering & Sciences*, vol. 15, pp. 1-16.

Atluri, S.N.; Shen, S. (2002a): The Meshless Local Petrov-Galerkin (MLPG) Method. Tech Science Press, 440 pages, Forsyth, GA.

Atluri, S.N.; Shen, S. (2002b): The meshless local Petrov-Galerkin (MLPG) method: A simple & lesscostly alternative to the finite element and boundary element methods. *CMES: Computer Modeling in Engineering & Sciences*, vol. 3, pp. 11-52.

Atluri, S.N.; Zhu, T. (1998): A new meshless local Petrov-Galerkin (MLPG) approach in computational mechanics. *Comput. Mech.*, vol. 22, pp. 117-127.

Atluri, S.N.; Zhu, T. (2000a): The meshless local Petrov-Galerkin (MLPG) approach for solving problems in elasto-statics. *Comput. Mech.*, vol.

25, pp. 169-179.

Atluri, S.N.; Zhu, T. (2000b): New concepts in meshless methods. *Int. J. Numer. Meth. Engng.*, vol. 47, pp. 537-556.

Aluru, N.R. (2000): A point collocation method based on reproducing kernel approximations. *Int. J. Numer. Meth. Engng.*, vol. 47, pp. 1083-1121.

Ballhause, D.; D'Ottavio, M.; Kröplin, B.; Carrera, E. (2005): A unified formulation to assess multilayered theories for piezoelectric plates. *Comput. Struct.*, vol. 83, pp. 1217-1235.

Batra, R.C.; Vidoli, S. (2002): Higher-order piezoelectric plate theory derived from a three-dimensional variational principle. *AIAA J.*, vol. 40, pp. 91-104.

Belytschko, T.; Krongauz, Y.; Organ, D.; Fleming, M.; Krysl, P. (1996): Meshless methods: An overview and recent developments. *Comput. Methods Appl. Mech. Engrg.*, vol. 139, pp. 3-47.

Belytschko, T.; Lu, Y.Y.; Gu, L. (1994): Element-Free Galerkin Methods. *Int. J. Numer. Meth. Engng.*, vol. 37, pp. 229-256.

Chen, J.S.; Pan, C.; Wu, C.T.; Liu, W.K. (1996): Reproducing kernel particle methods for large deformation analysis of non-linear structures. *Comput. Methods Appl. Mech. Engrg.*, vol. 139, pp. 195-227.

Chen, J.S.; Pan, C.; Roque, C.M.O.L.; Wang, H.P. (1998): Lagrangian reproducing kernel particle method for metal forming analysis. *Comput. Mech.*, vol. 22, pp. 289-307.

Dube, G.P.; Kapuria S.; Dumir, P.C. (1996): Exact piezothermoelastic solution of simply-supported orthotropic flat panel in cylindrical bending. *Int. J. Mech. Sci.*, vol. 38, pp. 1161-1177.

Han, Z.D.; Atluri, S.N. (2004a): Meshless local Petrov-Galerkin (MLPG) approaches for solving 3D problems in elasto-statics. *CMES: Computer Modeling in Engineering & Sciences*, vol. 6, pp. 169-188.

Han, Z.D.; Atluri, S.N. (2004b): Meshless local Petrov-Galerkin (MLPG) approaches for solving 3D problems in elasto-dynamics. *CMC: Computers, Materials & Continua*, vol. 1, pp. 129-140.

Han, Z.D.; Rajendran, A.M., Atluri, S.N. (2005): Meshless local Petrov-Galerkin (MLPG) approaches for solving nonlinear problems with large deformation and rotation. *CMES: Computer Modeling in Engineering & Sciences*, vol. 10, pp. 1-12.

Heyliger, P. (1994): Static behavior of laminated elastic/piezoelectric plates. *AIAA J.*, vol. 32, pp. 2481-2484.

Heyliger, P.; Brooks, S. (1995): Free vibration of piezoelectric laminates in cylindrical bending. *Int. J. Solids Struct.*, vol. 32, pp. 2945-2960.

Heyliger, P.; Brooks, S. (1996): Exact solutions for laminated piezoelectric plates in cylindrical bending. *J. Appl. Mech.*, vol. 63, pp. 903-910.

Jonnalagadda, K.D.; Blandford, G.E.; Tauchert, T.R. (1994): Piezothermoelastic composite plate analysis using first-order shear deformation theory. *Comput. & Struct.*, vol. 51, pp. 79-89.

Khdeir, A.A.; Aldraihem O.J. (2007): Analytical models and solutions of laminated composite piezoelectric plates. *Mech. Adv. Mater. Struct.*, vol. 14, pp. 67-80.

Lancaster, P.; Salkauakas, K. (1981): Surfaces generated by moving least squares methods. *Math. Comput.*, vol. 37, pp. 141-158.

Lee, J.S.; Jiang, L.Z. (1996): Exact electroelastic analysis of piezoelectric laminae via state space approach. *Int. J. Solids Struct.*, vol. 33, pp. 977-990.

Liu, W.K.; Jun, S.; Li, S.; Adee J.; Belytschko, T. (1995): Reproducing kernel particle methods for structural dynamics. *Int. J. Numer. Meth. Engng*. vol. 38, pp. 1655-1679.

Liu, W.K.; Jun, S.; Zhang, Y.F. (1995): Reproducing kernel particle methods. *Int. J. Numer. Meth. Engng*. vol. 20, pp. 1081-1106.

Lu, Y.Y.; Belytschko, T.; Gu, L. (1994): A new implementation of the element free Galerkin method. *Comput. Methods Appl. Mech. Engrg.*, vol. 113, pp. 397-414.

Mindlin, R. (1972): High frequency vibrations of piezoelectric crystal plates. *Int. J. Solids Struct.*, vol. 8, pp. 895-906.

Oñate, E.; Idelsohn, S.; Zienkiewicz, O.C.; Taylor, R.L. (1996): A finite point method in computational mechanics-Applications to convective transport and fluid flow. *Int. J. Numer. Meth. Engng.* vol. 39, pp. 3839-3866.

Pagano, N.J. (1969): Exact solutions for composites in cylindrical bending. *J. Compos. Mater.*, vol. 3, pp. 398-411.

Pagano, N.J. (1970): Exact solutions for rectangular bidirectional composites and sandwich plates. *J. Compos. Mater.*, vol. 4, pp. 20-34.

Pan, E. (2001): Exact solutions magneto-electro-elastic laminates in cylindrical bending. *Int. J. Solids Struct.*, vol. 40, pp. 6859-6876.

Pan, E.; Heyliger, P.R. (2003): Exact solution for simply supported and multilayered magneto-electro-elastic plates. *J. Appl. Mech.*, vol. 68, pp. 608-618.

Shan, Y.Y.; Shu, C.; Lu, Z.L. (2008): Application of local MQ-DQ method to solve 3D incompressible viscous flows with curved boundary. *CMES: Computer Modeling in Engineering & Sciences*, vol. 25, pp. 99-113.

Shu, C.; Ding, H.; Yeo, K.S. (2003): Local radial basis function-based differential quadrature method and its application to solve two-dimensional incompressible Navier-Stokes equations. *Comput. Methods Appl. Mech. Engrg.*, vol. 192, pp. 941-954.

Shu, C.; Ding, H.; Yeo, K.S. (2005): Computation of incompressible Navier-Stokes equations by local RBF-based differential quadrature method. *CMES: Computer Modeling in Engineering & Sciences*, vol. 7, pp. 195-205.

Shu, X. (2005): Free vibration of laminated piezoelectric composite plates based on an accurate theory. *Compos. Struct.*, vol. 67, pp. 375-382.

Tauchert, T.R. (1992): Piezothermoelastic behavior of a laminate. *J. Thermal Stresses*, vol. 15, pp. 25-37.

Tiersten, H.F., *Linear Piezoelectric Plate Vibrations*, Plenum Press, New York, 1969.

Vel, S.S.; Batra, R.C. (2000): Three-dimensional analytical solution for hybrid multilayered piezoelectric plates. *J. Appl. Mech.*, vol. 67, pp. 558-567.

Wu, C.P.; Lo, J.Y.; Chao, J.K. (2004): A three-dimensional asymptotic theory of laminated piezoelectric shells. *CMC: Computers, Materials & Continua*, vol. 2, pp.119-137.

Wu, C.P.; Lo, J.Y. (2006): An asymptotic theory for dynamic response of laminated piezoelectric shells. *Acta Mech.*, vol. 183, pp. 177-208.

Wu, C.P.; Syu, Y.S. (2007): Exact solution of functionally graded piezoelectric shells under cylindrical bending. *Int. J. Solids Struct.*, vol. 44, pp. 6450-6472.

Wu, C.P.; Syu, Y.S.; Lo, J.Y. (2007): Three-dimensional solutions of multilayered piezoelectric hollow cylinders by an asymptotic approach. *Int. J. Mech. Sci.*, vol. 49, pp. 669-689.

Wu, C.P.; Tsai, Y.H. (2008): Cylindrical bending vibration of functionally graded piezoelectric shells using the method of perturbation. *J. Eng. Math.*, in press.

Wu, W.X.; Shu, C.; Wang, C.M. (2008): Vibration analysis of arbitrarily shaped membranes using local radial basis function-based differential quadrature method. *J. Sound Vib.*, vol. 306, pp. 252-270.